Available online at www.sciencedirect.com
SCIENCE DIRECT®
Journal of Sound and Vibration 293 (2006) 380–408
JOURNAL OF SOUND AND VIBRATION
www.elsevier.com/locate/jsvi

Analytical and numerical studies of free vibrations of plate by imaginary-part BEM formulations

J.T. Chen[a,*], S.Y. Lin[a], Y.T. Lee[a], I.L. Chen[b]

[a]*Department of Harbor and River Engineering, National Taiwan Ocean University, Keelung, Taiwan*
[b]*Department of Naval Architecture, National Kaohsiung Marine University, Kaohsiung, Taiwan*

Received 12 July 2004; received in revised form 26 July 2005; accepted 7 October 2005
Available online 10 January 2006

Abstract

In this paper, the spurious solution of characteristic equation for the eigenproblems of a circular plate is studied in the continuous and discrete systems. Since any two boundary integral equations in the plate formulation (four equations) can be chosen, $6(C_2^4)$ options are considered instead of only two approaches (single-layer and double-layer methods, or singular and hypersingular equations). The occurring mechanism of the spurious solution for the circular plate in the imaginary-part formulations is studied analytically. For the continuous system, degenerate kernels for the fundamental solution and the Fourier series expansion for the boundary density are employed to derive the true and spurious solutions of characteristic equation analytically. For the discrete system, the degenerate kernels for the fundamental solution and circulants resulting from the circular boundary are employed to determine the spurious solution of characteristic equation. It is found that true solution for characteristic equation depends on the specified boundary condition while spurious one is embedded in each formulation. Also, we provide two methods (singular value decomposition updating technique and the Burton and Miller method) to suppress the occurrence of the spurious eigenvalues. A general-purpose program of imaginary-part boundary element method was developed for general cases. Several examples including circular and noncircular cases were demonstrated to check the validity of the formulation.

1. Introduction

For the simply-connected problems of interior acoustics or membrane, either the real-part or imaginary-part boundary element method (BEM) results in spurious solutions of characteristic equations. An analytical study for the spurious eigenvalues of a circular membrane was done [1] when the real-part BEM is employed to solve eigenproblem. De Mey [2,3], Yas'ko [4], Hutchinson and Wong [5–7] also employed only the real-part kernel to solve the membrane and plate vibrations free of the complex-valued computation in sacrifice of occurrence of spurious solutions. Wong and Hutchinson [8] have presented a direct BEM for plate vibration involving displacement, slope, moment and shear force. They were able to obtain numerical results for clamped plates by employing only the real-part BEM with obvious computational gains. However, this saving

*Corresponding author. Tel.: +886 2 24622192 ext. 6140 or 6177; fax: +886 2 24632375.
E-mail address: jtchen@mail.ntou.edu.tw (J.T. Chen).

0022-460X/$ - see front matter © 2005 Elsevier Ltd. All rights reserved.
doi:10.1016/j.jsv.2005.10.008

leads to spurious eigenvalues in addition to true ones for free vibration analysis. One has to investigate the mode shapes in order to identify and reject the spurious ones. Shaw [9] commented that using only the real-part kernel was incorrect since the characteristic equation must satisfy the real-part and imaginary-part equations at the same time. Hutchinson [10] replied that the claim of incorrectness was perhaps a little strong since the real-part BEM does not miss any true eigenvalue although the solution is contaminated by spurious ones according to numerical experiences. However, no proof was provided. Kuo et al. [1] and Chen et al. [11] have proved the existence of spurious solution through a circular membrane for the real-part and imaginary-part BEMs, respectively. If we usually need to look for the eigenmode as well as eigenvalue, the sorting for the spurious solutions pay a small overhead by identifying the mode shapes. Chen et al. [12] commented that the nodal line of spurious modes may be reasonable which could mislead the judgement of the true and spurious ones, since the true and spurious modes may have the same nodal line in case of different eigenvalues. This is the reason why Chen and his coworkers have developed several techniques, e.g., dual formulation [12], domain partition [13], singular value decomposition (SVD) updating technique [14], combined Helemholtz exterior equation formulation (CHEEF) method [15], for sorting out true and spurious eigenvalues. Niwa et al. [16] also stated that "One must take care to use the complete Green's function for outgoing waves, as attempts to use only the real (singular) or imaginary (regular) part separately will not provide the complete spectrum". As quoted from the reply of Hutchinson [10], this comment is not correct since the real-part BEM does not lose any true eigenvalue. The reason is that the real-part and imaginary-part kernels satisfy the Hilbert transform pair. They are not fully independent. To use both parts, real and imaginary kernels may be not economical in computation. Complete eigenspectrum is imbedded in either real or imaginary-part kernel. The spurious eigenvalues occur in two aspects: one is for the simply-connected eigenproblem by using the real-part or imaginary-part BEM; the other is for the multiply-connected eigenproblem even though the complex-valued BEM is utilized [17,18]. Based on the successful experiences for the eigenproblem of Laplace operator (membrane or acoustics), we intend to study the eigenproblem of biharmonic operator (plate).

In this paper, the spurious solution for the eigenproblems of a circular plate will be studied analytically and numerically. For saving the computational time and avoiding the singularity, we focus on the imaginary-part BEM only. Since any two boundary integral equations in the plate formulation (four equations) are chosen, $6(C_2^4)$ options can be considered instead of only two approaches (single-layer and double-layer methods, or singular and hypersingular equations) which are adopted for the eigenproblems of the membrane and acoustics. The occurring mechanism of the spurious solution for the circular plate in each formulation will be studied analytically in the continuous and discrete systems. Also, we will provide two methods (SVD updating technique and the Burton and Miller method) to suppress the occurrence of the spurious eigenvalues for the free vibration problems. Several examples, circular, rectangular and elliptical plates, will be demonstrated to check the validity of the proposed formulation.

2. Boundary integral equation and BEM for the free vibration of simply-connected plate

The governing equation for free flexural vibration of a uniform thin plate as shown in Fig. 1 is written as

$$\nabla^4 u(x) = \lambda^4 u(x), \quad x \in \Omega, \tag{1}$$

where u is the lateral displacement, $\lambda^4 = \omega^2 \rho_0 h/D$, λ is the frequency parameter, ω is the circular frequency, ρ_0 is the surface density, D is the flexural rigidity expressed as $D = Eh^3/12(1-\nu^2)$ in terms of Young's modulus E, the Poisson ratio ν and the plate thickness h, and Ω is the domain of the thin plate. The integral equations for the domain point can be derived from the Rayleigh–Green identity [19] as follows:

$$\begin{aligned} u(x) = & -\int_B U(s,x)v(s)\,\mathrm{d}B(s) + \int_B \Theta(s,x)m(s)\,\mathrm{d}B(s) \\ & -\int_B M(s,x)\theta(s)\,\mathrm{d}B(s) + \int_B V(s,x)u(s)\,\mathrm{d}B(s), \quad x \in \Omega, \end{aligned} \tag{2}$$

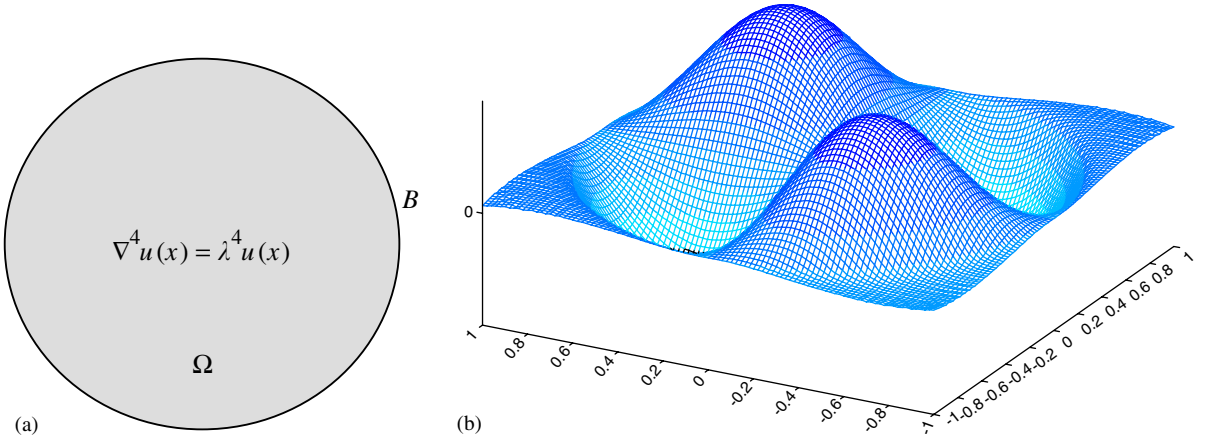

Fig. 1. Sketch of the problem. (a) Governing equation; (b) free flexural vibration.

$$\theta(x) = -\int_B U_\theta(s,x)v(s)\,\mathrm{d}B(s) + \int_B \Theta_\theta(s,x)m(s)\,\mathrm{d}B(s) - \int_B M_\theta(s,x)\theta(s)\,\mathrm{d}B(s) + \int_B V_\theta(s,x)u(s)\,\mathrm{d}B(s), \quad x \in \Omega, \tag{3}$$

$$m(x) = -\int_B U_m(s,x)v(s)\,\mathrm{d}B(s) + \int_B \Theta_m(s,x)m(s)\,\mathrm{d}B(s) - \int_B M_m(s,x)\theta(s)\,\mathrm{d}B(s) + \int_B V_m(s,x)u(s)\,\mathrm{d}B(s), \quad x \in \Omega, \tag{4}$$

$$v(x) = -\int_B U_v(s,x)v(s)\,\mathrm{d}B(s) + \int_B \Theta_v(s,x)m(s)\,\mathrm{d}B(s) - \int_B M_v(s,x)\theta(s)\,\mathrm{d}B(s) + \int_B V_v(s,x)u(s)\,\mathrm{d}B(s), \quad x \in \Omega, \tag{5}$$

where B is the boundary, u, θ, m and v mean the displacement, slope, normal moment, effective shear force, s and x are the source and field points, respectively, U, Θ, M and V kernel functions will be elaborated on later. The kernel function $U(s,x)$ is the fundamental solution $U_c(s,x)$ which satisfies

$$\nabla^4 U_c(s,x) - \lambda^4 U_c(s,x) = -\delta(x-s), \tag{6}$$

where $\delta(x-s)$ is the Dirac delta function. Considering the two singular solutions ($Y_0(\lambda r)$ and $K_0(\lambda r)$ which are the zeroth-order of second kind Bessel and modified Bessel functions, respectively) [8] and two regular solutions ($J_0(\lambda r)$ and $I_0(\lambda r)$, which are the zeroth-order of first kind Bessel and modified Bessel functions, respectively) in the fundamental solution, we have

$$U_c(s,x) = \frac{1}{8\lambda^2}\left[(Y_0(\lambda r) + \mathrm{i}J_0(\lambda r)) + \frac{2}{\pi}(K_0(\lambda r) + \mathrm{i}I_0(\lambda r))\right], \tag{7}$$

where $r \equiv |s-x|$ and $\mathrm{i}^2 = -1$. The other three kernels, $\Theta(s,x)$, $M(s,x)$ and $V(s,x)$, are defined as follows:

$$\Theta(s,x) = \mathscr{K}_\theta(U(s,x)), \tag{8}$$

$$M(s,x) = \mathscr{K}_m(U(s,x)), \tag{9}$$

$$V(s,x) = \mathscr{K}_v(U(s,x)), \tag{10}$$

where $\mathscr{K}_\theta(\cdot)$, $\mathscr{K}_m(\cdot)$ and $\mathscr{K}_v(\cdot)$ mean the operators defined by

$$\mathscr{K}_\theta(\cdot) \equiv \frac{\partial(\cdot)}{\partial n}, \tag{11}$$

$$\mathscr{K}_m(\cdot) \equiv \nu\nabla^2(\cdot) + (1-\nu)\frac{\partial^2(\cdot)}{\partial n^2}, \tag{12}$$

$$\mathscr{K}_v(\cdot) \equiv \frac{\partial\nabla^2(\cdot)}{\partial n} + (1-\nu)\frac{\partial}{\partial t}\left[\left(\frac{\partial^2(\cdot)}{\partial n\partial t}\right)\right], \tag{13}$$

where n and t are the normal vector and tangential vector, respectively. The operators $\mathscr{K}_\theta$, $\mathscr{K}_m$ and $\mathscr{K}_v$ can be applied to Θ, M and V kernels. The displacement, slope, normal moment and effective shear force are derived by

$$\theta(x) = \mathscr{K}_\theta(u(x)), \tag{14}$$

$$m(x) = \mathscr{K}_m(u(x)), \tag{15}$$

$$v(x) = \mathscr{K}_v(u(x)). \tag{16}$$

Once the field point x locates outside the domain, the null-field BIEs yield

$$\begin{aligned} 0 = &-\int_B U(s,x)v(s)\,\mathrm{d}B(s) + \int_B \Theta(s,x)m(s)\,\mathrm{d}B(s) \\ &-\int_B M(s,x)\theta(s)\,\mathrm{d}B(s) + \int_B V(s,x)u(s)\,\mathrm{d}B(s), \quad x \in \Omega^e, \end{aligned} \tag{17}$$

$$\begin{aligned} 0 = &-\int_B U_\theta(s,x)v(s)\,\mathrm{d}B(s) + \int_B \Theta_\theta(s,x)m(s)\,\mathrm{d}B(s) \\ &-\int_B M_\theta(s,x)\theta(s)\,\mathrm{d}B(s) + \int_B V_\theta(s,x)u(s)\,\mathrm{d}B(s), \quad x \in \Omega^e, \end{aligned} \tag{18}$$

$$\begin{aligned} 0 = &-\int_B U_m(s,x)v(s)\,\mathrm{d}B(s) + \int_B \Theta_m(s,x)m(s)\,\mathrm{d}B(s) \\ &-\int_B M_m(s,x)\theta(s)\,\mathrm{d}B(s) + \int_B V_m(s,x)u(s)\,\mathrm{d}B(s), \quad x \in \Omega^e, \end{aligned} \tag{19}$$

$$\begin{aligned} 0 = &-\int_B U_v(s,x)v(s)\,\mathrm{d}B(s) + \int_B \Theta_v(s,x)m(s)\,\mathrm{d}B(s) \\ &-\int_B M_v(s,x)\theta(s)\,\mathrm{d}B(s) + \int_B V_v(s,x)u(s)\,\mathrm{d}B(s), \quad x \in \Omega^e, \end{aligned} \tag{20}$$

where Ω^e is the complementary domain. Note that the null-field BIEs are not singular, since x and s never coincide. When the boundary is discretized into $2N$ constant elements, the linear algebraic equations of Eqs. (17)–(20) by moving the field point x close to the boundary B yield:

$$0 = [U]\{v\} + [\Theta]\{m\} + [M]\{\theta\} + [V]\{u\}, \tag{21}$$

$$0 = [U_\theta]\{v\} + [\Theta_\theta]\{m\} + [M_\theta]\{\theta\} + [V_\theta]\{u\}, \tag{22}$$

$$0 = [U_m]\{v\} + [\Theta_m]\{m\} + [M_m]\{\theta\} + [V_m]\{u\}, \tag{23}$$

$$0 = [U_v]\{v\} + [\Theta_v]\{m\} + [M_v]\{\theta\} + [V_v]\{u\}, \tag{24}$$

where $[U]$, $[\Theta]$, $[M]$, $[V]$, $[U_\theta]$, $[\Theta_\theta]$, $[M_\theta]$, $[V_\theta]$, $[U_m]$, $[\Theta_m]$, $[M_m]$, $[V_m]$, $[U_v]$, $[\Theta_v]$, $[M_v]$ and $[V_v]$ are the 16 influence matrices with the dimension of $2N \times 2N$, $\{u\}$, $\{\theta\}$, $\{m\}$ and $\{v\}$ are the vectors of boundary data with the dimension of $2N \times 1$. For the imaginary-part BEM, the kernel function $U(s,x)$ is the imaginary-part of the

fundamental solution

$$U(s,x) = \mathrm{Im}[U_c(s,x)] = \frac{1}{8\lambda^2}\left[(J_0(\lambda r) + \frac{2}{\pi}(I_0(\lambda r)\right]. \tag{25}$$

In order to obtain the true and spurious characteristic equations for plate vibration in the imaginary-part BEM, the degenerate kernel, Fourier series and circulants are adopted in the continuous and discrete systems of a circular plate. Three cases (clamped, simply-supported and free plates) are demonstrated analytically in the continuous and the discrete systems, respectively, in the following subsections.

2.1. Continuous system

2.1.1. Case 1. Clamped circular plate

For the clamped circular plate ($u = 0$ and $\theta = 0$) with a radius a, we can obtain the characteristic equation in the continuous formulation. The moment and shear force, $m(s)$ and $v(s)$, are expanded into Fourier series by

$$m(s) = \sum_{n=0}^{\infty}(p_n^c \cos(n\overline{\phi}) + q_n^c \sin(n\overline{\phi})), \quad s \in B, \tag{26}$$

$$v(s) = \sum_{n=0}^{\infty}(a_n^c \cos(n\overline{\phi}) + b_n^c \sin(n\overline{\phi})), \quad s \in B, \tag{27}$$

where the superscript "c" denotes the clamped case, $\overline{\phi}$ is the angle on the circular boundary, a_n^c, b_n^c, p_n^c and q_n^c are the undetermined Fourier coefficients. Substituting Eqs. (26) and (27) into Eqs. (17) and (18), we have

$$\begin{aligned} 0 = & -\int_0^{2\pi} U(s,x)\left[\sum_{n=0}^{\infty}(a_n^c \cos(n\overline{\phi}) + b_n^c \sin(n\overline{\phi}))\right] \mathrm{d}B(s) \\ & + \int_0^{2\pi} \Theta(s,x)\left[\sum_{n=0}^{\infty}(p_n^c \cos(n\overline{\phi}) + q_n^c \sin(n\overline{\phi}))\right] \mathrm{d}B(s), \quad x \in B, \end{aligned} \tag{28}$$

$$\begin{aligned} 0 = & -\int_0^{2\pi} U_\theta(s,x)\left[\sum_{n=0}^{\infty}(a_n^c \cos(n\overline{\phi}) + b_n^c \sin(n\overline{\phi}))\right] \mathrm{d}B(s) \\ & + \int_0^{2\pi} \Theta_\theta(s,x)\left[\sum_{n=0}^{\infty}(p_n^c \cos(n\overline{\phi}) + q_n^c \sin(n\overline{\phi}))\right] \mathrm{d}B(s), \quad x \in B. \end{aligned} \tag{29}$$

The kernel functions, $U(s,x)$, $\Theta(s,x)$, $U_\theta(s,x)$ and $\Theta_\theta(s,x)$, are expanded by using the expansion formulae,

$$J_0(\lambda r) = \begin{cases} J_0^i(\lambda r) = \sum\limits_{m=-\infty}^{\infty} J_m(\lambda\overline{\rho})J_m(\lambda\rho)\cos(m(\overline{\phi}-\phi)), & \overline{\rho} > \rho, \\ J_0^e(\lambda r) = \sum\limits_{m=-\infty}^{\infty} J_m(\lambda\rho)J_m(\lambda\overline{\rho})\cos(m(\overline{\phi}-\phi)), & \rho > \overline{\rho}, \end{cases} \tag{30}$$

$$I_0(\lambda r) = \begin{cases} I_0^i(\lambda r) = \sum\limits_{m=-\infty}^{\infty} (-1)^m I_m(\lambda\overline{\rho})I_m(\lambda\rho)\cos(m(\overline{\phi}-\phi)), & \overline{\rho} > \rho, \\ I_0^e(\lambda r) = \sum\limits_{m=-\infty}^{\infty} (-1)^m I_m(\lambda\rho)I_m(\lambda\overline{\rho})\cos(m(\overline{\phi}-\phi)), & \rho > \overline{\rho}, \end{cases} \tag{31}$$

where J_m and I_m denote the first kind of the mth-order Bessel and modified Bessel functions. The superscripts "i" and "e" denote the interior point ($\overline{\rho} > \rho$) and the exterior point ($\overline{\rho} < \rho$), $s = (\overline{\rho}, \overline{\phi})$ and $x = (\rho, \phi)$ are the polar coordinates of s and x, respectively. In this case, $\overline{\rho} = \rho = a$ and $\mathrm{d}B(s) = a\,\mathrm{d}\overline{\phi}$ for the circular plate with a radius a. Similarly, the other kernels can also be expanded into degenerate forms. By using the degenerate kernels into Eq. (28) and by employing the orthogonality condition of the Fourier series, the Fourier

coefficients a_n^c, b_n^c, p_n^c and q_n^c satisfy

$$p_n^c = \frac{1}{\lambda}\frac{[J_n(\lambda a)J_n(\lambda a)+\frac{2}{\pi}(-1)^n I_n(\lambda a)I_n(\lambda a)]}{[J_n(\lambda a)J_n'(\lambda a)+\frac{2}{\pi}(-1)^n I_n(\lambda a)I_n'(\lambda a)]}\, a_n^c, \quad n=0,1,2,\ldots, \tag{32}$$

$$q_n^c = \frac{1}{\lambda}\frac{[J_n(\lambda a)J_n(\lambda a)+\frac{2}{\pi}(-1)^n I_n(\lambda a)I_n(\lambda a)]}{[J_n(\lambda a)J_n'(\lambda a)+\frac{2}{\pi}(-1)^n I_n(\lambda a)I_n'(\lambda a)]}\, b_n^c, \quad n=0,1,2,\ldots. \tag{33}$$

Similarly, Eq. (29) yields,

$$p_n^c = \frac{1}{\lambda}\frac{[J_n'(\lambda a)J_n(\lambda a)+\frac{2}{\pi}(-1)^n I_n'(\lambda a)I_n(\lambda a)]}{[J_n'(\lambda a)J_n'(\lambda a)+\frac{2}{\pi}(-1)^n I_n'(\lambda a)I_n'(\lambda a)]}\, a_n^c, \quad n=0,1,2,\ldots, \tag{34}$$

$$q_n^c = \frac{1}{\lambda}\frac{[J_n'(\lambda a)J_n(\lambda a)+\frac{2}{\pi}(-1)^n I_n'(\lambda a)I_n(\lambda a)]}{[J_n'(\lambda a)J_n'(\lambda a)+\frac{2}{\pi}(-1)^n I_n'(\lambda a)I_n'(\lambda a)]}\, b_n^c, \quad n=0,1,2,\ldots. \tag{35}$$

To obtain the nontrivial data for the generalized coefficients of a_n^c, p_n^c, b_n^c and q_n^c, we derive the characteristic equation by using either Eqs. (32) and (34) or Eqs. (33) and (35)

$$\frac{J_n(\lambda a)J_n(\lambda a)+\frac{2}{\pi}(-1)^n I_n(\lambda a)I_n(\lambda a)}{J_n(\lambda a)J_n'(\lambda a)+\frac{2}{\pi}(-1)^n I_n(\lambda a)I_n'(\lambda a)} = \frac{J_n'(\lambda a)J_n(\lambda a)+\frac{2}{\pi}(-1)^n I_n'(\lambda a)I_n(\lambda a)}{J_n'(\lambda a)J_n'(\lambda a)+\frac{2}{\pi}(-1)^n I_n'(\lambda a)I_n'(\lambda a)}. \tag{36}$$

After collecting the terms by using the recurrence relations of the Bessel function, Eq. (36) is simplified to

$$[I_{n+1}(\lambda a)J_n(\lambda a)+J_{n+1}(\lambda a)I_n(\lambda a)]\{I_{n+1}(\lambda a)J_n(\lambda a)+J_{n+1}(\lambda a)I_n(\lambda a)\}=0. \tag{37}$$

The former part in Eq. (37) inside the square bracket is the spurious solution while the latter part inside the curly bracket is found to be the true solution after comparing with the exact solution [20]. In this case, it is interesting to find that the true and spurious solutions are the same. We can also comment that no spurious eigenvalue occurs although spurious multiplicity may appear. Eq. (37) is similar to the characteristic equation $J_n(\lambda a)J_n(\lambda a)=0$ for the membrane [11] when the imaginary-part BEM is employed.

2.1.2. Case 2. Simply-supported circular plate

Following the same procedure of case 1, we have

$$\frac{J_n(\lambda a)J_n(\lambda a)+\frac{2}{\pi}(-1)^n I_n(\lambda a)I_n(\lambda a)}{J_n(\lambda a)\alpha_n^J(\lambda a)+\frac{2}{\pi}(-1)^n I_n(\lambda a)\alpha_n^I(\lambda a)} = \frac{J_n'(\lambda a)J_n(\lambda a)+\frac{2}{\pi}(-1)^n I_n'(\lambda a)I_n(\lambda a)}{J_n'(\lambda a)\alpha_n^J(\lambda a)+\frac{2}{\pi}(-1)^n I_n'(\lambda a)\alpha_n^I(\lambda a)}, \tag{38}$$

where

$$\alpha_n^J(\lambda a) = \lambda^2 J_n''(\lambda a)+\nu\left[\frac{1}{a}\lambda J_n'(\lambda a)-\left(\frac{n}{a}\right)^2 J_n(\lambda a)\right], \tag{39}$$

$$\alpha_n^I(\lambda a) = \lambda^2 I_n''(\lambda a)+\nu\left[\frac{1}{a}\lambda I_n'(\lambda a)-\left(\frac{n}{a}\right)^2 I_n(\lambda a)\right]. \tag{40}$$

After collecting the terms by using the recurrence relations of the Bessel function, Eq. (38) is simplified to

$$[I_{n+1}(\lambda a)J_n(\lambda a)+J_{n+1}(\lambda a)I_n(\lambda a)]$$

$$\{(1-\nu)I_n(\lambda a)J_{n+1}(\lambda a)+I_{n+1}(\lambda a)J_n(\lambda a)-2\lambda a I_n(\lambda a)J_n(\lambda a)\}=0. \tag{41}$$

The former part in Eq. (41) inside the square bracket is the spurious solution while the latter part inside the curly bracket is found to be the true solution after comparing with the exact solution [20]. The spurious solution in Eq. (41) is the same as the former one in Eq. (37) for the clamped case by using the imaginary-part BEM.

2.1.3. Case 3. Free circular plate

Following the same procedure of case 1, we have

$$\frac{[J_n(\lambda a)\alpha_n^J(\lambda a)+\frac{2}{\pi}(-1)^n I_n(\lambda a)\alpha_n^I(\lambda a)]}{[J_n(\lambda a)\beta_n^J(\lambda a)+\frac{2}{\pi}(-1)^n I_n(\lambda a)\beta_n^I(\lambda a)+\frac{1-v}{a}[J_n(\lambda a)\gamma_n^J(\lambda a)+\frac{2}{\pi}(-1)^n I_n(\lambda a)\gamma_n^I(\lambda a)]]} = \frac{[J_n'(\lambda a)J_n(\lambda a)+\frac{2}{\pi}(-1)^n I_n'(\lambda a)I_n(\lambda a)]}{[J_n'(\lambda a)\beta_n^J(\lambda a)+\frac{2}{\pi}(-1)^n I_n'(\lambda a)\beta_n^I(\lambda a)+\frac{1-v}{a}[J_n'(\lambda a)\gamma_n^J(\lambda a)+\frac{2}{\pi}(-1)^n I_n'(\lambda a)\gamma_n^I(\lambda a)]]}, \tag{42}$$

where

$$\beta_n^J(\lambda a)=\lambda^3 J_n'''(\lambda a)+v\left[\frac{1}{a}\lambda^2 J_n''(\lambda a)-\left(\frac{n}{a}\right)^2\lambda J_n'(\lambda a)-\frac{1}{a^2}\lambda J_n'(\lambda a)+\left(\frac{2n^2}{a^3}\right)J_n(\lambda a)\right], \tag{43}$$

$$\beta_n^I(\lambda a)=\lambda^3 I_n'''(\lambda a)+v\left[\frac{1}{a}\lambda^2 I_n''(\lambda a)-\left(\frac{n}{a}\right)^2\lambda I_n'(\lambda a)-\frac{1}{a^2}\lambda I_n'(\lambda a)+\left(\frac{2n^2}{a^3}\right)I_n(\lambda a)\right], \tag{44}$$

$$\gamma_n^J(\lambda a)=-n^2\left[\frac{1}{a^2}J_n(\lambda a)+\frac{\lambda}{a}J_n'(\lambda a)\right], \tag{45}$$

$$\gamma_n^I(\lambda a)=-n^2\left[\frac{1}{a^2}I_n(\lambda a)+\frac{\lambda}{a}I_n'(\lambda a)\right]. \tag{46}$$

After collecting the terms by using the recurrence relations of the Bessel function, Eq. (42) is simplified to

$$\begin{aligned}&[I_{n+1}(\lambda a)J_n(\lambda a)+J_{n+1}(\lambda a)I_n(\lambda a)]\{\lambda a(1-v)[-4n^2(n-1)I_n(\lambda a)J_n(\lambda a)-2\lambda^2a^2I_{n+1}(\lambda a)J_{n+1}(\lambda a)]\\&\quad+2n\lambda^2a^2(1-v)(1-n)(I_{n+1}(\lambda a)J_n(\lambda a)-I_n(\lambda a)J_{n+1}(\lambda a))\\&\quad+[n^2(1-v)^2(n^2-1)+\lambda^4a^4](I_{n+1}(\lambda a)J_n(\lambda a)+I_n(\lambda a)J_{n+1}(\lambda a))\}=0.\end{aligned} \tag{47}$$

The former part in Eq. (47) inside the square bracket is the spurious solution which also appears in the clamped and simply-supported cases. It is found that the spurious solutions of Eqs. (37), (41) and (47) are not different since the same formulation (null-field integral formulation of Eqs. (17) and (18)) is used. This indicates that spurious solution depends on the formulation instead of the specified boundary condition. The results of true solution were summaried in Table 1, and the results of spurious solution were rearranged in Table 2.

2.2. Discrete system

2.2.1. Case 1. Clamped circular plate

For the clamped circular plate ($u=0$ and $\theta=0$) with a radius a, Eqs. (21) and (22) can be rewritten as

$$\{0\}=[U]\{v\}+[\Theta]\{m\}, \tag{48}$$

$$\{0\}=[U_\theta]\{v\}+[\Theta_\theta]\{m\}. \tag{49}$$

Table 1
True solution for a circular plate ($a=1$)

	True eigensolution for circular plate
Clamped circular plate	$I_{\ell+1}J_\ell+I_\ell J_{\ell+1}=0$
Simply-supported circular plate	$(1-v)(I_\ell J_{\ell+1}+I_{\ell+1}J_\ell)-2\lambda I_\ell J_\ell=0$
Free circular plate	$\lambda(1-v)[-4\ell^2(\ell-1)I_\ell J_\ell-2\lambda^2 I_{\ell+1}J_{\ell+1}]+2\ell\lambda^2(1-v)(1-\ell)(I_{\ell+1}J_\ell-I_\ell J_{\ell+1})$ $+[\ell^2(1-v)^2(\ell^2-1)+\lambda^4](I_{\ell+1}J_\ell+I_\ell J_{\ell+1})=0$

$\ell=0,\pm1,\pm2,\pm3,\ldots$.

Table 2
Spurious solution by using the six formulations in the imaginary-part BEM

	Spurious eigensolution in the imaginary-part BEM
u,θ formulation	$I_{\ell+1}J_\ell + I_\ell J_{\ell+1} = 0$
u,m formulation	$(1-\nu)(I_\ell J_{\ell+1} + I_{\ell+1}J_\ell) - 2\lambda\rho I_\ell J_\ell = 0$
u,v formulation	$\ell^2(1-\nu)(I_\ell J_{\ell+1} + I_{\ell+1}J_\ell) - 2\lambda\rho\ell I_\ell J_\ell + \lambda^2\rho^2(I_\ell J_{\ell+1} - I_{\ell+1}J_\ell) = 0$
θ,m formulation	$\ell^2(1-\nu)(I_\ell J_{\ell+1} + I_{\ell+1}J_\ell) - 2\lambda\rho\ell I_\ell J_\ell + \lambda^2\rho^2(I_\ell J_{\ell+1} - I_{\ell+1}J_\ell) = 0$
θ,v formulation	$2\lambda\rho(\ell^2 I_\ell J_\ell - \lambda^2\rho^2 I_{\ell+1}J_{\ell+1}) + 2\lambda^2\rho^2\ell(I_{\ell+1}J_\ell - I_\ell J_{\ell+1}) - \ell^2(1-\nu)](I_{\ell+1}J_\ell + I_\ell J_{\ell+1}) = 0$
m,v formulation	$\lambda\rho(1-\nu)[-4\ell^2(\ell-1)I_\ell J_\ell - 2\lambda^2\rho^2 I_{\ell+1}J_{\ell+1}] + 2\ell\lambda^2\rho^2(1-\nu)(1-\ell)(I_{\ell+1}J_\ell - I_\ell J_{\ell+1}) +$ $[\ell^2(1-\nu)^2(\ell^2-1) + \lambda^4\rho^4](I_{\ell+1}J_\ell + I_\ell J_{\ell+1}) = 0$

$\ell = 0, \pm1, \pm2, \pm3, \ldots$.

By assembling Eqs. (48) and (49) together, we have

$$[\mathrm{SM}^c]\begin{Bmatrix} v \\ m \end{Bmatrix} = \{0\}, \tag{50}$$

where the superscript "c" denotes the clamped case and

$$[\mathrm{SM}^c] = \begin{bmatrix} U & \Theta \\ U_\theta & \Theta_\theta \end{bmatrix}_{4N\times 4N}. \tag{51}$$

For the existence of nontrivial solution of $\{{}^{v}_{m}\}$, the determinant of the matrix versus eigenvalue must be zero, i.e.,

$$\det[\mathrm{SM}^c] = 0. \tag{52}$$

Since the rotation symmetry is preserved for a circular boundary, the influence matrices for the discrete system are found to be the circulants. The eigenvalues ($\mu_\ell^{[U]}$) of the 16 influence matrices ($[U]$) for the discrete system can be obtained by using the property of the circulant.

$$\mu_\ell^{[U]} = -\frac{\pi a}{4\lambda^2}\left[J_\ell(\lambda a)J_\ell(\lambda a) + \frac{2}{\pi}(-1)^\ell I_\ell(\lambda a)I_\ell(\lambda a)\right], \quad \ell = 0, \pm1, \pm2, \ldots, \pm(N-1), N. \tag{53}$$

Similarly, we have

$$\mu_\ell^{[\Theta]} = \frac{\pi a}{4\lambda}\left[J_\ell(\lambda a)J'_\ell(\lambda a) + \frac{2}{\pi}(-1)^\ell I_\ell(\lambda a)I'_\ell(\lambda a)\right], \quad \ell = 0, \pm1, \pm2, \ldots, \pm(N-1), N, \tag{54}$$

$$\kappa_\ell^{[U]} = -\frac{\pi a}{4\lambda}\left[J'_\ell(\lambda a)J_\ell(\lambda a) + \frac{2}{\pi}(-1)^\ell I'_\ell(\lambda a)I_\ell(\lambda a)\right], \quad \ell = 0, \pm1, \pm2, \ldots, \pm(N-1), N, \tag{55}$$

$$\kappa_\ell^{[\Theta]} = \frac{\pi a}{4}\left[J'_\ell(\lambda a)J'_\ell(\lambda a) + \frac{2}{\pi}(-1)^\ell I'_\ell(\lambda a)I'_\ell(\lambda a)\right], \quad \ell = 0, \pm1, \pm2, \ldots, \pm(N-1), N, \tag{56}$$

where $\mu_\ell^{[\Theta]}$, $\kappa_\ell^{[U]}$ and $\kappa_\ell^{[\Theta]}$ are the eigenvalues of $[\Theta]$, $[U_\theta]$ and $[\Theta_\theta]$ matrices, respectively. Since the four matrices $[U]$, $[\Theta]$, $[U_\theta]$ and $[\Theta_\theta]$ are all symmetric circulants, they can be expressed as

$$[U] = \Phi\Sigma_U\Phi^{-1}, \tag{57}$$

$$[\Theta] = \Phi\Sigma_\Theta\Phi^{-1}, \tag{58}$$

$$[U_\theta] = \Phi\Sigma_{U_\theta}\Phi^{-1}, \tag{59}$$

$$[\Theta_\theta] = \Phi\Sigma_{\Theta_\theta}\Phi^{-1}, \tag{60}$$

where

$$\Sigma_U = \mathrm{diag}(\mu_0^{[U]}, \mu_1^{[U]}, \mu_{-1}^{[U]}, \ldots, \mu_{(N-1)}^{[U]}, \mu_{-(N-1)}^{[U]}, \mu_N^{[U]}), \tag{61}$$

$$\Sigma_\Theta = \mathrm{diag}(\mu_0^{[\Theta]}, \mu_1^{[\Theta]}, \mu_{-1}^{[\Theta]}, \ldots, \mu_{(N-1)}^{[\Theta]}, \mu_{-(N-1)}^{[\Theta]}, \mu_N^{[\Theta]}), \tag{62}$$

$$\Sigma_{U_\theta} = \mathrm{diag}(\kappa_0^{[U]}, \kappa_1^{[U]}, \kappa_{-1}^{[U]}, \ldots, \kappa_{(N-1)}^{[U]}, \kappa_{-(N-1)}^{[U]}, \kappa_N^{[U]}), \tag{63}$$

$$\Sigma_{\Theta_\theta} = \mathrm{diag}(\kappa_0^{[\Theta]}, \kappa_1^{[\Theta]}, \kappa_{-1}^{[\Theta]}, \ldots, \kappa_{(N-1)}^{[\Theta]}, \kappa_{-(N-1)}^{[\Theta]}, \kappa_N^{[\Theta]}) \tag{64}$$

and

$$\Phi = \frac{1}{\sqrt{2N}} \begin{bmatrix} 1 & 1 & 0 & \cdots & 1 & 0 & 1 \\ 1 & \cos\left(\frac{2\pi}{2N}\right) & \sin\left(\frac{2\pi}{2N}\right) & \cdots & \cos\left(\frac{2\pi(N-1)}{2N}\right) & \sin\left(\frac{2\pi(N-1)}{2N}\right) & \cos\left(\frac{2\pi N}{2N}\right) \\ 1 & \cos\left(\frac{4\pi}{2N}\right) & \sin\left(\frac{4\pi}{2N}\right) & \cdots & \cos\left(\frac{4\pi(N-1)}{2N}\right) & \sin\left(\frac{4\pi(N-1)}{2N}\right) & \cos\left(\frac{4\pi N}{2N}\right) \\ \vdots & \vdots & \vdots & \ddots & \vdots & \vdots & \vdots \\ 1 & \cos\left(\frac{2\pi(2N-2)}{2N}\right) & \sin\left(\frac{2\pi(2N-2)}{2N}\right) & \cdots & \cos\left(\frac{\pi(4N-4)(N-1)}{2N}\right) & \sin\left(\frac{\pi(4N-4)(N-1)}{2N}\right) & \cos\left(\frac{\pi(4N-4)(N)}{2N}\right) \\ 1 & \cos\left(\frac{2\pi(2N-1)}{2N}\right) & \sin\left(\frac{2\pi(2N-1)}{2N}\right) & \cdots & \cos\left(\frac{\pi(4N-2)(N-1)}{2N}\right) & \sin\left(\frac{\pi(4N-2)(N-1)}{2N}\right) & \cos\left(\frac{\pi(4N-2)(N)}{2N}\right) \end{bmatrix}_{2N\times 2N}. \tag{65}$$

By employing Eqs. (57)–(60) for Eq. (51), we have

$$[\mathrm{SM}^c] = \begin{bmatrix} \Phi\Sigma_U\Phi^{-1} & \Phi\Sigma_\Theta\Phi^{-1} \\ \Phi\Sigma_{U_\theta}\Phi^{-1} & \Phi\Sigma_{\Theta_\theta}\Phi^{-1} \end{bmatrix}_{4N\times 4N}, \tag{66}$$

Eq. (66) can be reformulated into

$$[\mathrm{SM}^c] = \begin{bmatrix} \Phi & 0 \\ 0 & \Phi \end{bmatrix} \begin{bmatrix} \Sigma_U & \Sigma_\Theta \\ \Sigma_{U_\theta} & \Sigma_{\Theta_\theta} \end{bmatrix} \begin{bmatrix} \Phi^{-1} & 0 \\ 0 & \Phi^{-1} \end{bmatrix}. \tag{67}$$

By using the property of the determinant, the determinant of $[\mathrm{SM}^c]_{4N\times 4N}$ is

$$\det[\mathrm{SM}^c] = \det \begin{bmatrix} \Sigma_U & \Sigma_\Theta \\ \Sigma_{U_\theta} & \Sigma_{\Theta_\theta} \end{bmatrix} = \prod_{\ell=-(N-1)}^{N} (\mu_\ell^{[U]}\kappa_\ell^{[\Theta]} - \mu_\ell^{[\Theta]}\kappa_\ell^{[U]}), \tag{68}$$

since Φ is orthogonal. By employing Eqs. (53)–(56) for Eq. (68), we have

$$\begin{aligned} \det[\mathrm{SM}^c] = & \prod_{\ell=-(N-1)}^{N} \frac{\pi^2 a^2}{16\lambda^2} \\ & \times \left\{ \left[J_\ell(\lambda a) J_\ell(\lambda a) + \frac{2}{\pi}(-1)^\ell I_\ell(\lambda a) I_\ell(\lambda a) \right] \left[J'_\ell(\lambda a) J'_\ell(\lambda a) + \frac{2}{\pi}(-1)^\ell I'_\ell(\lambda a) I'_\ell(\lambda a) \right] \right. \\ & \left. - \left[J_\ell(\lambda a) J'_\ell(\lambda a) + \frac{2}{\pi}(-1)^\ell I_\ell(\lambda a) I'_\ell(\lambda a) \right] \left[J'_\ell(\lambda a) J_\ell(\lambda a) + \frac{2}{\pi}(-1)^\ell I'_\ell(\lambda a) I_\ell(\lambda a) \right] \right\}. \end{aligned} \tag{69}$$

By using the recurrence relations of the Bessel function, Eq. (69) is simplified into

$$\begin{aligned} \det[\mathrm{SM}^c] = & \prod_{\ell=-(N-1)}^{N} \frac{\pi a^2}{8\lambda^2} [I_{\ell+1}(\lambda a) J_\ell(\lambda a) + J_{\ell+1}(\lambda a) I_\ell(\lambda a)] \\ & \times \{ I_{\ell+1}(\lambda a) J_\ell(\lambda a) + J_{\ell+1}(\lambda a) I_\ell(\lambda a) \} = 0. \end{aligned} \tag{70}$$

Zero determinant in Eq. (70) implies that the characteristic equation is

$$[I_{\ell+1}(\lambda a)J_\ell(\lambda a)+J_{\ell+1}(\lambda a)I_\ell(\lambda a)]\{I_{\ell+1}(\lambda a)J_\ell(\lambda a)+J_{\ell+1}(\lambda a)I_\ell(\lambda a)\}=0,$$
$$\ell=0,\pm1,\pm2,\ldots,\pm(N-1),N. \tag{71}$$

After comparing with the analytical solution for the clamped circular plate [20], the true solution for the continuous system is obtained by approaching N in the discrete system to infinity. The result of Eq. (71) in the discrete system matches well with Eq. (37) in the continuous system.

2.2.2. Case 2. Simply-supported circular plate

For the simply-supported circular plate ($u=0$ and $m=0$) with a radius a, we have

$$[\mathrm{SM}^s]=\begin{bmatrix} U & M \\ U_\theta & M_\theta \end{bmatrix}_{4N\times 4N}, \tag{72}$$

where the superscript "s" denotes the simply-supported case. By using the property of the determinant and the recurrence relations of the Bessel function, the determinant of $[\mathrm{SM}^s]_{4N\times4N}$ is simplified into

$$\det[\mathrm{SM}^s]=\prod_{\ell=-(N-1)}^{N}\frac{\pi a}{8\lambda^2}[I_{\ell+1}(\lambda a)J_\ell(\lambda a)+J_{\ell+1}(\lambda a)I_\ell(\lambda a)]$$
$$\times\{(1-v)I_\ell(\lambda a)J_{n+1}(\lambda a)+I_{n+1}(\lambda a)J_\ell(\lambda a)-2\lambda a I_\ell(\lambda a)J_\ell(\lambda a)\}=0. \tag{73}$$

Zero determinant in Eq. (73) implies that the characteristic equation is

$$[I_{\ell+1}(\lambda a)J_\ell(\lambda a)+J_{\ell+1}(\lambda a)I_\ell(\lambda a)]\{(1-v)I_\ell(\lambda a)J_{n+1}(\lambda a)+I_{n+1}(\lambda a)J_\ell(\lambda a)-2\lambda a I_\ell(\lambda a)J_\ell(\lambda a)\}=0,$$
$$\ell=0,\pm1,\pm2,\ldots,\pm(N-1),N. \tag{74}$$

After comparing with the analytical solution for the simply-supported circular plate [20], the true solution for the continuous system is obtained by approaching N in the discrete system to infinity. The result of Eq. (74) in the discrete system matches well with Eq. (41) in the continuous system.

2.2.3. Case 3. Free circular plate

For the free circular plate ($m=0$ and $v=0$) with a radius a, we have

$$[\mathrm{SM}^f]=\begin{bmatrix} M & V \\ M_\theta & V_\theta \end{bmatrix}_{4N\times 4N}, \tag{75}$$

where the superscript "f" denotes the free case. By using the property of the determinant and the recurrence relations of the Bessel function, the determinant of $[\mathrm{SM}^f]_{4N\times4N}$ is simplified into

$$\det[\mathrm{SM}^f]=\prod_{\ell=-(N-1)}^{N}\frac{\pi a}{8\lambda^2}[I_{\ell+1}(\lambda a)J_\ell(\lambda a)+J_{\ell+1}(\lambda a)I_\ell(\lambda a)]$$
$$\times\{\lambda a(1-v)[-4\ell^2(\ell-1)]I_\ell(\lambda a)J_\ell(\lambda a)-2\lambda^2a^2I_{\ell+1}(\lambda a)J_{\ell+1}(\lambda a)]$$
$$+2\ell\lambda^2a^2(1-v)(1-\ell)(I_{\ell+1}(\lambda a)J_\ell(\lambda a)-I_\ell(\lambda a)J_{\ell+1}(\lambda a))$$
$$+[\ell^2(1-v)^2(\ell^2-1)+\lambda^4a^4](I_{\ell+1}(\lambda a)J_\ell(\lambda a)+I_\ell(\lambda a)J_{\ell+1}(\lambda a))\}=0. \tag{76}$$

Zero determinant in Eq. (76) implies that the characteristic equation is

$$[I_{\ell+1}(\lambda a)J_\ell(\lambda a)+J_{\ell+1}(\lambda a)I_\ell(\lambda a)]\{\lambda a(1-v)[-4\ell^2(\ell-1)I_\ell(\lambda a)J_\ell(\lambda a)-2\lambda^2a^2I_{\ell+1}(\lambda a)J_{\ell+1}(\lambda a)]$$
$$+2\ell\lambda^2a^2(1-v)(1-\ell)(I_{\ell+1}(\lambda a)J_\ell(\lambda a)-I_\ell(\lambda a)J_{\ell+1}(\lambda a))$$
$$+[\ell^2(1-v)^2(\ell^2-1)+\lambda^4a^4](I_{\ell+1}(\lambda a)J_\ell(\lambda a)+I_\ell(\lambda a)J_{\ell+1}(\lambda a))\}=0,$$
$$\ell=0,\pm1,\pm2,\ldots,\pm(N-1),N. \tag{77}$$

After comparing with the analytical solution for the free circular plate [20], the true solution for the continuous system is obtained by approaching N in the discrete system to infinity. The result of Eq. (77) in the discrete system matches well with Eq. (47) in the continuous system. After comparing Eq. (71) with Eqs. (74) and (77), the same spurious solution of characteristic equation ($[I_{\ell+1}(\lambda a)J_\ell(\lambda a)+J_{\ell+1}(\lambda a)I_\ell(\lambda a)]=0$) is simultaneously embedded in the u, θ formulation no matter what the boundary condition is.

Since any two equations in the plate formulation (Eqs. (21)–(24)) are chosen, $6(C_2^4)$ options of the formulation can be considered. If we choose different combinations of the formulae for any one of the clamped, simply-supported or free circular plate cases, we obtain the same true solution but different spurious solutions. At the same time, the clamped, simply-supported and free circular plates result in the same spurious solution, once the same formulation is chosen. The occurrence of spurious solution only depends on the formulation instead of the specified boundary condition. True solution depends on the specified boundary condition instead of the formulation. All the results are summarized in Tables 1 and 2. After comparing Table 1 with Table 2, it is found that spurious and true solutions are the same not only when using the essential boundary integral equations ($u-\theta$ formulation) for the essential boundary conditions (clamped) but also the natural boundary integral equations ($m-v$ formulation) for the natural boundary conditions (free). It is similar to membrane problem [11].

To the authors' best knowledge, the occurrence of the spurious mode and rigid body mode are both attributed to the rank-deficiency of the influence matrix. The zero-energy modes produce numerical instability in FEM for the reduced-order Gaussian quadrature. In the FEM, the zero-energy mode can separate into two parts: one is the rigid body mode (physically realizable) and the other is the hour-glass mode (mathematically realizable). Further research have been done and they were addressed in Ref. [21].

3. Treatment of the spurious eigenvalues for simply-connected characteristic problems

3.1. SVD updating technique

3.1.1. Continuous system

A conventional approach to detect the nonunique solution is the criterion of satisfying all Eqs. (21)–(24) at the same time in the imaginary-part BEM. For the clamped plate ($u=0$ and $\theta=0$), the moment and shear force ($m(s)$ and $v(s)$), are expanded into Fourier series as shown in Eqs. (26) and (27). By substituting the degenerate kernels into Eqs. (17)–(18) and by employing the orthogonality condition of the Fourier series, the Fourier coefficients a_n^c, b_n^c, p_n^c and q_n^c satisfy Eqs. (32)–(35). If we employ Eq. (19) to solve the same characteristic problem, we obtain the Fourier coefficients a_n^c, b_n^c, p_n^c and q_n^c satisfying

$$p_n^c=\frac{[\alpha_n^J(\lambda a)J_n(\lambda a)+\frac{2}{\pi}\alpha_n^I(\lambda a)I_n(\lambda a)]}{[\alpha_n^J(\lambda a)J_n'(\lambda a)+\frac{2}{\pi}\alpha_n^I(\lambda a)I_n'(\lambda a)]}\,a_n^c,\quad n=0,1,2,\ldots, \tag{78}$$

$$q_n^c=\frac{[\alpha_n^J(\lambda a)J_n(\lambda a)+\frac{2}{\pi}\alpha_n^I(\lambda a)I_n(\lambda a)]}{[\alpha_n^J(\lambda a)J_n'(\lambda a)+\frac{2}{\pi}\alpha_n^I(\lambda a)I_n'(\lambda a)]}\,b_n^c,\quad n=0,1,2,\ldots. \tag{79}$$

Similarly, Eq. (20) yields,

$$p_n^c=\frac{[\beta_n^J(\lambda a)J_n(\lambda a)+\frac{2}{\pi}\beta_n^I(\lambda a)(\lambda a)I_n(\lambda a)+\frac{1-\nu}{a}[\gamma_n^J(\lambda a)J_n(\lambda a)+\frac{2}{\pi}\gamma_n^I(\lambda a)I_n(\lambda a)]]}{[\beta_n^J(\lambda a)J_n'(\lambda a)+\frac{2}{\pi}\beta_n^I(\lambda a)(\lambda a)I_n'(\lambda a)+\frac{1-\nu}{a}[\gamma_n^J(\lambda a)J_n'(\lambda a)+\frac{2}{\pi}\gamma_n^I(\lambda a)I_n'(\lambda a)]]}\,a_n^c,\quad n=0,1,2,\ldots, \tag{80}$$

$$q_n^c=\frac{[\beta_n^J(\lambda a)J_n(\lambda a)+\frac{2}{\pi}\beta_n^I(\lambda a)(\lambda a)I_n(\lambda a)+\frac{1-\nu}{a}[\gamma_n^J(\lambda a)J_n(\lambda a)+\frac{2}{\pi}\gamma_n^I(\lambda a)I_n(\lambda a)]]}{[\beta_n^J(\lambda a)J_n'(\lambda a)+\frac{2}{\pi}\beta_n^I(\lambda a)(\lambda a)I_n'(\lambda a)+\frac{1-\nu}{a}[\gamma_n^J(\lambda a)J_n'(\lambda a)+\frac{2}{\pi}\gamma_n^I(\lambda a)I_n'(\lambda a)]]}\,b_n^c,\quad n=0,1,2,\ldots. \tag{81}$$

For the true solution of characteristic equation

$$\{I_{n+1}(\lambda a)J_n(\lambda a)+J_{n+1}(\lambda a)I_n(\lambda a)\}=0,\quad n=0,\pm1,\pm2,\ldots,\pm(N-1),N, \tag{82}$$

Eqs. (32), (34), (78) and (80) are simplified to

$$p_n^c = \frac{I(\lambda a)}{\lambda I_n'(\lambda a)}\, a_n^c, \quad n = 0, 1, 2, \ldots . \tag{83}$$

In this case, we obtain the nontrivial data of the true boundary mode in the column vector form by employing Eq. (83) as shown below:

$$\begin{Bmatrix} a_0^c \\ p_0^c \\ a_1^c \\ b_1^c \\ p_1^c \\ q_1^c \\ \vdots \\ a_n^c \\ b_n^c \\ p_n^c \\ q_n^c \\ \vdots \\ a_{2N}^c \\ b_{2N}^c \\ p_{2N}^c \\ q_{2N}^c \end{Bmatrix} = \begin{Bmatrix} 0 \\ 0 \\ 0 \\ 0 \\ 0 \\ 0 \\ \vdots \\ 1 \\ 0 \\ I_n(\lambda a))/\lambda I_n'(\lambda a) \\ 0 \\ \vdots \\ 0 \\ 0 \\ 0 \\ 0 \end{Bmatrix} a_n^c + \begin{Bmatrix} 0 \\ 0 \\ 0 \\ 0 \\ 0 \\ 0 \\ \vdots \\ 0 \\ 1 \\ 0 \\ I_n(\lambda a))/\lambda I_n'(\lambda a) \\ \vdots \\ 0 \\ 0 \\ 0 \\ 0 \end{Bmatrix} b_n^c, \tag{84}$$

where a_n^c and b_n^c are arbitrary. The column vector of the true boundary modes is the same by using any one of Eqs. (32), (34), (78) and (80). In case of the spurious eigenvalue, Eqs. (32), (34), (78) and (80) cannot obtain the common term. After collecting any two terms of Eqs. (32), (34), (78) and (80) by using the recurrence relations of the Bessel function, it is found that all the results can be simplified to six different spurious solutions as shown in Table 2. The same true solution is commonly imbedded in the six imaginary-part formulations. A possible way to obtain the nontrivial data for the generalized coefficients is only the common one (true solution in Eq. (82)) to be satisfied.

This indicates that only the true solution of the clamped circular plate is sorted out since it is simultaneously embedded in the six imaginary-part formulations. The result matches well with Eqs. (37) and (71) in the continuous and discrete systems, respectively. Since we solve the same problem by using the imaginary-part BEM, only the true solution of the clamped circular plate is sorted out for the same reason that the true solution is simultaneously embedded in the six imaginary-part formulations. This is the mathematical meaning of the SVD technique of updating term in the continuous system. We will apply the SVD updating technique in the discrete system.

3.1.2. Discrete system

In the discrete system, the approach to detect the spurious characteristic solution is the criterion of satisfying all Eqs. (21)–(24) at the same time in the imaginary-part BEM. For the clamped plate ($u = 0$ and $\theta = 0$), Eqs. (21)–(22) reduce to

$$[\mathrm{SM}_1^c]\begin{Bmatrix} v \\ m \end{Bmatrix} = 0, \tag{85}$$

where

$$[\mathrm{SM}_1^c] = \begin{bmatrix} U & \Theta \\ U_\theta & \Theta_\theta \end{bmatrix}. \tag{86}$$

Similarly, Eqs. (23) and (24) yield

$$[\mathrm{SM}_2^c]\begin{Bmatrix} v \\ m \end{Bmatrix} = 0, \tag{87}$$

where

$$[\mathrm{SM}_2^c] = \begin{bmatrix} U_m & \Theta_m \\ U_v & \Theta_v \end{bmatrix}. \tag{88}$$

Since the imaginary-part BEM misses the real-part information, we reconstruct the independent equation by differentiation. To obtain an overdetermined system, we can combine Eqs. (85) and (87) by using the SVD technique of updating term as shown below:

$$[C]\begin{Bmatrix} v \\ m \end{Bmatrix} = 0, \tag{89}$$

where

$$[C] = \begin{bmatrix} \mathrm{SM}_1^c \\ \mathrm{SM}_2^c \end{bmatrix}_{8N\times 4N}. \tag{90}$$

Since the characteristic equation is nontrivial, the rank of the matrix $[C]$ must be smaller than $4N$. The $4N$ singular values for the matrix $[C]$ must have at least one zero value. The explicit form for the matrix $[C]$ is decomposed into

$$[C] = \begin{bmatrix} \Phi & 0 & 0 & 0 \\ 0 & \Phi & 0 & 0 \\ 0 & 0 & \Phi & 0 \\ 0 & 0 & 0 & \Phi \end{bmatrix}_{8N\times 8N} \begin{bmatrix} \Sigma_U & \Sigma_\Theta \\ \Sigma_{U_\theta} & \Sigma_{\Theta_\theta} \\ \Sigma_{U_m} & \Sigma_{\Theta_m} \\ \Sigma_{U_v} & \Sigma_{\Theta_v} \end{bmatrix}_{8N\times 4N} \begin{bmatrix} \Phi^{\mathrm{T}} & 0 \\ 0 & \Phi^{\mathrm{T}} \end{bmatrix}_{4N\times 4N}. \tag{91}$$

Based on the equivalence between the SVD technique and the least-squares method in mathematical essence [22], the least squares form leads to

$$[C]^{\mathrm{T}}[C] = \begin{bmatrix} \Phi & 0 \\ 0 & \Phi \end{bmatrix}_{4N\times 4N} [D]_{4N\times 4N} \begin{bmatrix} \Phi & 0 \\ 0 & \Phi \end{bmatrix}^{\mathrm{T}}_{4N\times 4N}, \tag{92}$$

where

$$[D] = \begin{bmatrix} \Sigma_U & \Sigma_{U_\theta} & \Sigma_{U_m} & \Sigma_{U_v} \\ \Sigma_\Theta & \Sigma_{\Theta_\theta} & \Sigma_{\Theta_m} & \Sigma_{\Theta_v} \end{bmatrix}_{4N\times 8N} \begin{bmatrix} \Sigma_U & \Sigma_\Theta \\ \Sigma_{U_\theta} & \Sigma_{\Theta_\theta} \\ \Sigma_{U_m} & \Sigma_{\Theta_m} \\ \Sigma_{U_v} & \Sigma_{\Theta_v} \end{bmatrix}_{8N\times 4N}. \tag{93}$$

If the determinant of the matrix $[C]^{\mathrm{T}}[C]$ is zero, we can obtain the nontrivial solution. Since Φ is orthogonal, the determinant of the matrix $[C]^{\mathrm{T}}[C]$ is equal to the determinant of the matrix $[D]$. By calculating the determinant of the matrix $[D]$, we have

$$\begin{aligned} \det[D] = \prod_{\ell=-(N-1)}^{N} & [(\mu_\ell^{[U]}\kappa_\ell^{[\Theta]} - \mu_\ell^{[\Theta]}\kappa_\ell^{[U]})^2 + (\mu_\ell^{[U]}\zeta_\ell^{[\Theta]} - \mu_\ell^{[\Theta]}\zeta_\ell^{[U]})^2 + (\mu_\ell^{[U]}\delta_\ell^{[\Theta]} - \mu_\ell^{[\Theta]}\delta_\ell^{[U]})^2 \\ & + (\kappa_\ell^{[U]}\zeta_\ell^{[\Theta]} - \kappa_\ell^{[\Theta]}\zeta_\ell^{[U]})^2 + (\kappa_\ell^{[U]}\delta_\ell^{[\Theta]} - \kappa_\ell^{[\Theta]}\delta_\ell^{[U]})^2 + (\zeta_\ell^{[U]}\delta_\ell^{[\Theta]} - \zeta_\ell^{[\Theta]}\delta_\ell^{[U]})^2], \end{aligned} \tag{94}$$

where $\zeta_\ell^{[U]}$, $\zeta_\ell^{[\Theta]}$, $\delta_\ell^{[\Theta]}$ and $\delta_\ell^{[U]}$ are the eigenvalues of the matrices $[U_m]$, $[\Theta_m]$, $[U_v]$ and $[\Theta_v]$, respectively. The only possibility for the zero determinant of the matrix $[D]$ occurs when the six terms, $(\mu_\ell^{[U]}\kappa_\ell^{[\Theta]}-\mu_\ell^{[\Theta]}\kappa_\ell^{[U]})$, $(\mu_\ell^{[U]}\zeta_\ell^{[\Theta]}-\mu_\ell^{[\Theta]}\zeta_\ell^{[U]})$, $(\mu_\ell^{[U]}\delta_\ell^{[\Theta]}-\mu_\ell^{[\Theta]}\delta_\ell^{[U]})$, $(\kappa_\ell^{[U]}\zeta_\ell^{[\Theta]}-\kappa_\ell^{[\Theta]}\zeta_\ell^{[U]})$, $(\kappa_\ell^{[U]}\delta_\ell^{[\Theta]}-\kappa_\ell^{[\Theta]}\delta_\ell^{[U]})$ and $(\zeta_\ell^{[U]}\delta_\ell^{[\Theta]}-\zeta_\ell^{[\Theta]}\delta_\ell^{[U]})$ are all zeros simultaneously for the same ℓ. Here we find that the six terms exactly result in the six different spurious solutions as shown in Table 2, and the same true solution is commonly imbedded in the six imaginary-part formulations. A possible way for the zero determinant of the matrix $[D]$ is the common term (true solution in Eq. (82)) to be satisfied.

This indicates that only the true solution of the clamped circular plate is sorted out in the SVD updating matrix since it is simultaneously embedded in the six imaginary-part formulations (see Eq. (94)). The result matches well with Eqs. (37) and (71) in the continuous and discrete systems, respectively. Since we solve the same problem by using the imaginary-part BEM, only the true solution of the clamped circular plate is sorted out for the same reason that the true solution is simultaneously embedded in the six imaginary-part formulations.

3.2. Burton and Miller method and the complex-valued BEM

In the exterior acoustics of Helmholtz equation by using the dual BEM, Burton and Miller [23] utilized the product of hypersingular equation with an imaginary constant and added the singular equation to deal with the fictitious-frequency problem which results in a non-uniqueness solution. We will extend this concept to suppress the appearance of spurious solution in the imaginary-part BEM.

3.2.1. Continuous system

For the clamped circular plate with a radius a, combination of Eqs. (17) and (19) with an imaginary number by using the imaginary-part BEM yields

$$0=-\int_B [U(s,x)+\mathrm{i}U_m(s,x)]v(s)\,\mathrm{d}B(s)+\int_B [\Theta(s,x)+\mathrm{i}\Theta_m(s,x)]m(s)\,\mathrm{d}B(s). \tag{95}$$

Similarly, Eqs. (18) and (20) yield,

$$0=-\int_B [U_\theta(s,x)+\mathrm{i}U_v(s,x)]v(s)\,\mathrm{d}B(s)+\int_B [\Theta_\theta(s,x)+\mathrm{i}\Theta_v(s,x)]m(s)\,\mathrm{d}B(s). \tag{96}$$

The moment and shear force, $m(s)$ and $v(s)$, are expanded into Fourier series as shown in Eqs. (26) and (27). By using the degenerate kernels into Eq. (95) and by employing the orthogonality condition of the Fourier series, the Fourier coefficients a_n^c, b_n^c, p_n^c and q_n^c satisfy

$$p_n^c=\frac{[J_n(\lambda a)J_n(\lambda a)+\frac{2}{\pi}I_n(\lambda a)I_n(\lambda a)]+i[\alpha_n^J(\lambda a)J_n(\lambda a)+\frac{2}{\pi}\alpha_n^I(\lambda a)I_n(\lambda a)]}{[J_n(\lambda a)J_n'(\lambda a)+\frac{2}{\pi}I_n(\lambda a)I_n'(\lambda a)]+i[\alpha_n^J(\lambda a)J_n'(\lambda a)+\frac{2}{\pi}\alpha_n^I(\lambda a)I_n'(\lambda a)]}\,a_n^c,\quad n=0,1,2,\ldots, \tag{97}$$

$$q_n^c=\frac{[J_n(\lambda a)J_n(\lambda a)+\frac{2}{\pi}I_n(\lambda a)I_n(\lambda a)]+i[\alpha_n^J(\lambda a)J_n(\lambda a)+\frac{2}{\pi}\alpha_n^I(\lambda a)I_n(\lambda a)]}{[J_n(\lambda a)J_n'(\lambda a)+\frac{2}{\pi}I_n(\lambda a)I_n'(\lambda a)]+i[\alpha_n^J(\lambda a)J_n'(\lambda a)+\frac{2}{\pi}\alpha_n^I(\lambda a)I_n'(\lambda a)]}\,b_n^c,\quad n=0,1,2,\ldots. \tag{98}$$

Similarly, Eq. (96) yields,

$$p_n^c=\frac{\lambda[J_n'(\lambda a)J_n(\lambda a)+\frac{2}{\pi}I_n'(\lambda a)I_n(\lambda a)]}{\lambda[J_n'(\lambda a)J_n'(\lambda a)+\frac{2}{\pi}I_n'(\lambda a)I_n'(\lambda a)]}$$
$$\frac{+i[\beta_n^J(\lambda a)J_n(\lambda a)+\frac{2}{\pi}\beta_n^I(\lambda a)I_n(\lambda a)+\frac{1-\nu}{a}[\gamma_n^Y(\lambda a)J_n(\lambda a)+\frac{2}{\pi}\gamma_n^K(\lambda a)(\lambda a)I_n(\lambda a)]]}{+i[\beta_n^J(\lambda a)J_n'(\lambda a)+\frac{2}{\pi}\beta_n^I(\lambda a)I_n'(\lambda a)+\frac{1-\nu}{a}[\gamma_n^Y(\lambda a)J_n'(\lambda a)+\frac{2}{\pi}\gamma_n^K(\lambda a)I_n'(\lambda a)]]}\,a_n^c,\quad n=0,1,2,\ldots, \tag{99}$$

$$q_n^c=\frac{\lambda[J_n'(\lambda a)J_n(\lambda a)+\frac{2}{\pi}I_n'(\lambda a)I_n(\lambda a)]}{\lambda[J_n'(\lambda a)J_n'(\lambda a)+\frac{2}{\pi}I_n'(\lambda a)I_n'(\lambda a)]}$$
$$\frac{+i[\beta_n^J(\lambda a)J_n(\lambda a)+\frac{2}{\pi}\beta_n^I(\lambda a)I_n(\lambda a)+\frac{1-\nu}{a}[\gamma_n^Y(\lambda a)J_n(\lambda a)+\frac{2}{\pi}\gamma_n^K(\lambda a)(\lambda a)I_n(\lambda a)]]}{+i[\beta_n^J(\lambda a)J_n'(\lambda a)+\frac{2}{\pi}\beta_n^I(\lambda a)I_n'(\lambda a)+\frac{1-\nu}{a}[\gamma_n^Y(\lambda a)J_n'(\lambda a)+\frac{2}{\pi}\gamma_n^K(\lambda a)I_n'(\lambda a)]]}\,b_n^c,\quad n=0,1,2,\ldots. \tag{100}$$

To obtain the nontrivial data for the generalized coefficients of a_n^c, p_n^c, b_n^c and q_n^c, we derive the characteristic equation by using either Eqs. (97) and (99) or Eqs. (98) and (100)

$$\begin{aligned}&\frac{[J_n(\lambda a)J_n(\lambda a)+\frac{2}{\pi}I_n(\lambda a)I_n(\lambda a)]+i[\alpha_n^J(\lambda a)J_n(\lambda a)+\frac{2}{\pi}\alpha_n^I(\lambda a)I_n(\lambda a)]}{[J_n(\lambda a)J_n'(\lambda a)+\frac{2}{\pi}I_n(\lambda a)I_n'(\lambda a)]+i[\alpha_n^J(\lambda a)J_n'(\lambda a)+\frac{2}{\pi}\alpha_n^I(\lambda a)I_n'(\lambda a)]}\\ &\quad=\frac{\lambda[J_n'(\lambda a)J_n(\lambda a)+\frac{2}{\pi}I_n'(\lambda a)I_n(\lambda a)]}{\lambda[J_n'(\lambda a)J_n'(\lambda a)+\frac{2}{\pi}I_n'(\lambda a)I_n'(\lambda a)]}\\ &\quad\quad\frac{+i[\beta_n^J(\lambda a)J_n(\lambda a)+\frac{2}{\pi}\beta_n^I(\lambda a)I_n(\lambda a)+\frac{1-v}{a}[\gamma_n^J(\lambda a)J_n(\lambda a)+\frac{2}{\pi}\gamma_n^I(\lambda a)(\lambda a)I_n(\lambda a)]]}{+i[\beta_n^J(\lambda a)J_n'(\lambda a)+\frac{2}{\pi}\beta_n^I(\lambda a)I_n'(\lambda a)+\frac{1-v}{a}[\gamma_n^J(\lambda a)J_n'(\lambda a)+\frac{2}{\pi}\gamma_n^I(\lambda a)I_n'(\lambda a)]]}.\end{aligned}\tag{101}$$

After collecting the terms by using the recurrence relations of the Bessel function, Eq. (101) is simplified to

$$[A(\lambda)+\mathrm{i}B(\lambda)]\{I_{n+1}(\lambda a)J_n(\lambda a)+J_{n+1}(\lambda a)I_n(\lambda a)\}=0.\tag{102}$$

Since the term $[A(\lambda)+\mathrm{i}B(\lambda)]$ is never zero for any λ, we can obtain the true eigenvalues by using the imaginary-part BEM in conjunction with the Burton and Miller concept. Nevertheless, the method fails if we combine the u, θ and m, v formulations or u, v and θ, m formulations. The reason is that the u, v and θ, m formulation have the same spurious solution. It occurs that $A(\lambda)$ ($B(\lambda)$) may be always zero for any λ, this results in the spurious eigenvalue since the other coefficient $B(\lambda)$ ($A(\lambda)$) may be zero. Only the combination of u, m and θ, v imaginary-part formulation yields the true eigenvalues. All the explicit forms of the $[A(\lambda)+\mathrm{i}B(\lambda)]$ are shown in Table 3 by using the imaginary-part BEM.

Since the imaginary-part BEM misses the real-part information, we can reconstruct the independent equation by adding the other imaginary-part BEM multiplied by an imaginary unit. By employing the Burton and Miller concept to combine the real and imaginary-part for the same formulation (e.g. u, θ formulae), the complex-valued BEM can be treated as a special case of Burton and Miller method. This indicates that Burton and Miller method and the complex-valued BEM are mathematical equivalent if we choose the same formulation (e.g. u, θ formulae). To extract the true solution, we construct the imaginary-part formulation (u, θ formulae) and combine with m, v formulae by multiplying an imaginary unit.

3.2.2. Discrete system

By combining Eqs. (85) and (87) with an imaginary number in the imaginary-part BEM, we have

$$[[\mathrm{SM}_1^c]+\mathrm{i}[\mathrm{SM}_2^c]]\begin{Bmatrix}v\\ m\end{Bmatrix}=0.\tag{103}$$

The determinant of the $[\mathrm{SM}_1^c]+\mathrm{i}[\mathrm{SM}_2^c]$ is obtained by using the circulant as

$$\det[[\mathrm{SM}_1^c]+\mathrm{i}[\mathrm{SM}_2^c]]=\prod_{\ell=-(N-1)}^{N}[A(\lambda)+\mathrm{i}B(\lambda)]\{I_{\ell+1}(\lambda a)J_\ell(\lambda a)+J_{\ell+1}(\lambda a)I_\ell(\lambda a)\}.\tag{104}$$

The comment in the continuous system for Eq. (102) can be extended to the discrete system.

4. Numerical results and discussions

4.1. Circular plate (clamped (c), simply-supported (s) and free (F) boundary conditions)

A circular plate with a radius of 1 m ($a=1$ m) and the Poisson ratio $v=0.33$ are considered. The boundary is uniformly discretized into 10 constant elements. Since any two equations in the plate formulation (Eqs. (21)–(24)) are chosen, $6(C_2^4)$ options of the formulation can be considered. By using the imaginary-part BEM, the numerical results are shown below.

4.1.1. True and spurious eigenvalues in the imaginary-part BEM

Based on the six imaginary-part formulations, the determinant of [SM] versus frequency parameter λ for the clamped, simply-supported and free circular plates are shown in Figs. 2–4, respectively. In each figure, we find

Table 3
The terms of $A(\lambda)+iB(\lambda)$ by using the imaginary-part BEM in conjunction with the Burton and Miller concept for the simply-connected circular plate

(a) $A(\lambda)$

u,θ formulation	$\dfrac{(-1)^n\{J_{n+1}\{[n^4(-1+\nu)^2+2n\lambda^2(-1+\nu)\rho^2+(1+\lambda^4)\rho^4-n^2(1-2\nu+\nu^2-2\lambda^2\rho^2+2\lambda^2\nu\rho^2)]I_n+2\lambda^3(-1+\nu)\rho^3I_{n+1}\}}{32\pi\lambda^2\rho^4}$ $+\dfrac{(-1)^n\{J_n\{4(-1+n)n^2\lambda(-1+\nu)\rho I_n+\{n^4(-1+\nu)^2-2n\lambda^2(-1+\nu)\rho^2+(1+\lambda^4)\rho^4-n^2[1+\nu^2+2\lambda^2\rho^2-2\nu(1+\lambda^2\rho^2)]\}I_{n+1}\}\}}{32\pi\lambda^4\rho^4}$
u,m formulation	$\dfrac{(-1)^n\{J_{n+1}\{[-n^2(-1+\nu)+2n\lambda^2\rho^2+(-1+\nu)\rho^2]I_n+2\lambda^3\rho^3I_{n+1}\}\}+(-1)^n\{J_n\{2\lambda\rho(-n^2+\rho^2)I_n+[-n^2(-1+\nu)-2n\lambda^2\rho^2+(-1+\nu)\rho^2]I_{n+1}\}\}}{32\pi\lambda^2\rho^3}$
u,v formulation	0
θ,m formulation	$\dfrac{(-1)^n\{J_{n+1}\{[n^2(-1+\nu)-2n\lambda^2\rho^2+(-1+\nu)\rho^2]I_n-2\lambda^3\rho^3I_{n+1}\}+(-1)^n\{J_n\{2\lambda\rho(n^2+\rho^2)I_n+[n^2(-1+\nu)+2n\lambda^2\rho^2+(-1+\nu)\rho^2]I_{n+1}\}\}}{32\pi\lambda^2\rho^4}$
θ,v formulation	$\dfrac{(-1)^n\{[n^2(-1+\nu)-\lambda^2\rho^2]J_{n+1}I_n\}+(-1)^n\{J_n\{2n\lambda\rho I_n+[n^2(-1+\nu)+\lambda^2\rho^2]I_{n+1}\}\}}{16\pi\lambda^2\rho^2}$
m,v formulation	0

(b) $B(\lambda)$

u,θ formulation	0
u,m formulation	$\dfrac{(-1)^n\{[n^2(-1+\nu)-\lambda^2\rho^2]J_{n+1}I_n\}+(-1)^n\{J_n\{2n\lambda\rho I_n+[n^2(-1+\nu)+\lambda^2\rho^2]I_{n+1}\}\}}{16\pi\lambda^2\rho^2}$
u,v formulation	$\dfrac{(-1)^n\{J_{n+1}\{[n^2(-1+\nu)-2n\lambda^2\rho^2+(-1+\nu)\rho^2]I_n-2\lambda^3\rho^3I_{n+1}\}+(-1)^n\{J_n\{2\lambda\rho(n^2+\rho^2)I_n+[n^2(-1+\nu)+2n\lambda^2\rho^2+(-1+\nu)\rho^2]I_{n+1}\}\}}{32\pi\lambda^2\rho^4}$
θ,mformulation	0
θ,v formulation	$\dfrac{(-1)^n\{J_{n+1}\{[-n^2(-1+\nu)+2n\lambda^2\rho^2+(-1+\nu)\rho^2]I_n+2\lambda^3\rho^3I_{n+1}\}\}+(-1)^n\{J_n\{2\lambda\rho(-n^2+\rho^2)I_n+[-n^2(-1+\nu)-2n\lambda^2\rho^2+(-1+\nu)\rho^2]I_{n+1}\}\}}{32\pi\lambda^2\rho^3}$
m,v formulation	$\dfrac{(-1)^n\{J_{n+1}\{[n^4(-1+\nu)^2+2n\lambda^2(-1+\nu)\rho^2+(1+\lambda^4)\rho^4-n^2(1-2\nu+\nu^2-2\lambda^2\rho^2+2\lambda^2\nu\rho^2)]I_n+2\lambda^3(-1+\nu)\rho^3I_{n+1}\}}{32\pi\lambda^2\rho^4}$ $+\dfrac{(-1)^n\{J_n\{4(-1+n)n^2\lambda(-1+\nu)\rho I_n+\{n^4(-1+\nu)^2-2n\lambda^2(-1+\nu)\rho^2+(1+\lambda^4)\rho^4-n^2[1+\nu^2+2\lambda^2\rho^2-2\nu(1+\lambda^2\rho^2)]\}I_{n+1}\}\}}{32\pi\lambda^2\rho^4}$

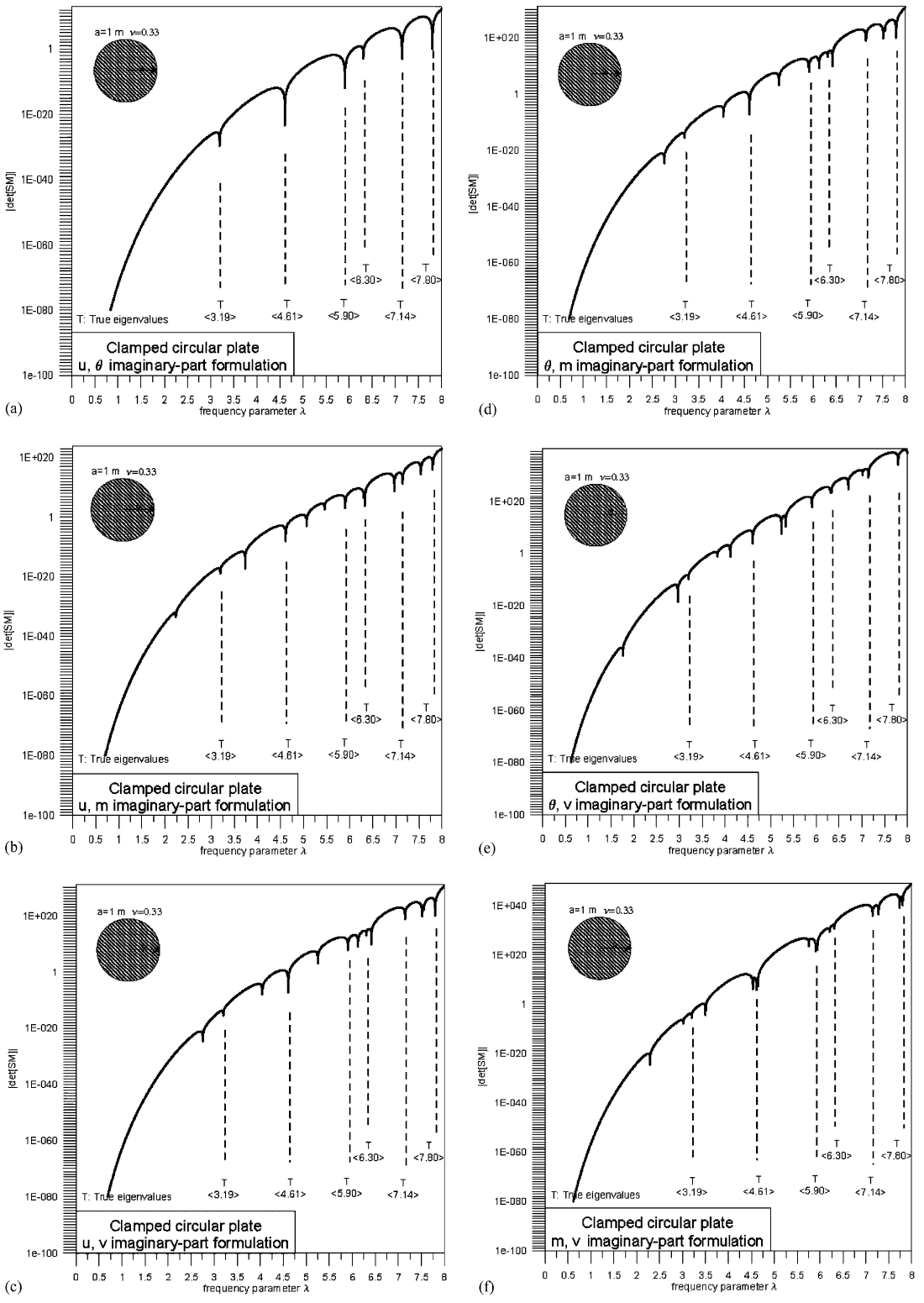

Fig. 2. The absolute value of determinant for $[SM^c]$ versus frequency parameter λ for the clamped circular plate using the six imaginary-part formulations.

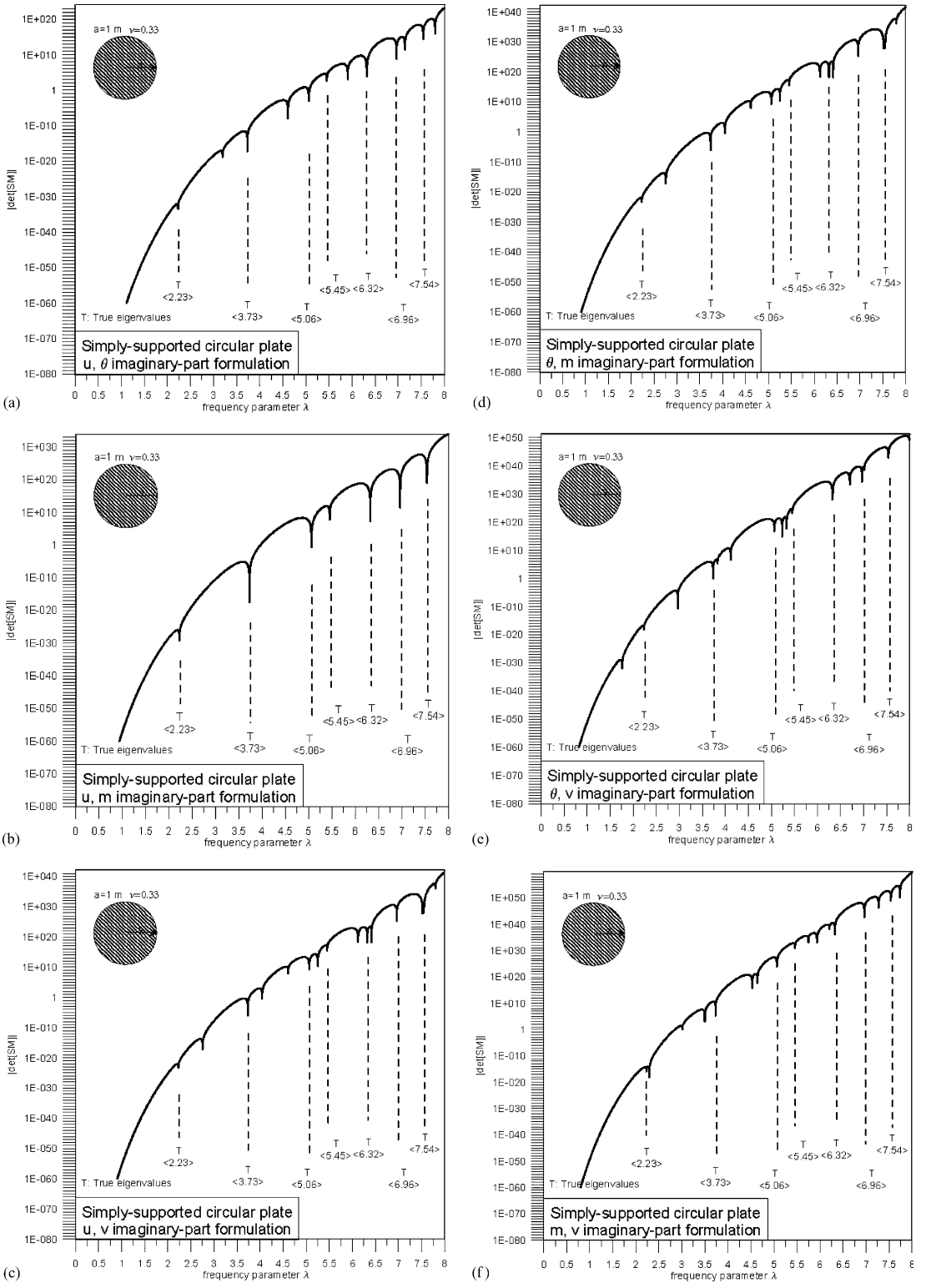

Fig. 3. The absolute value of determinant for $[SM^s]$ versus frequency parameter λ for the simply-supported circular plate using the six imaginary-part formulations.

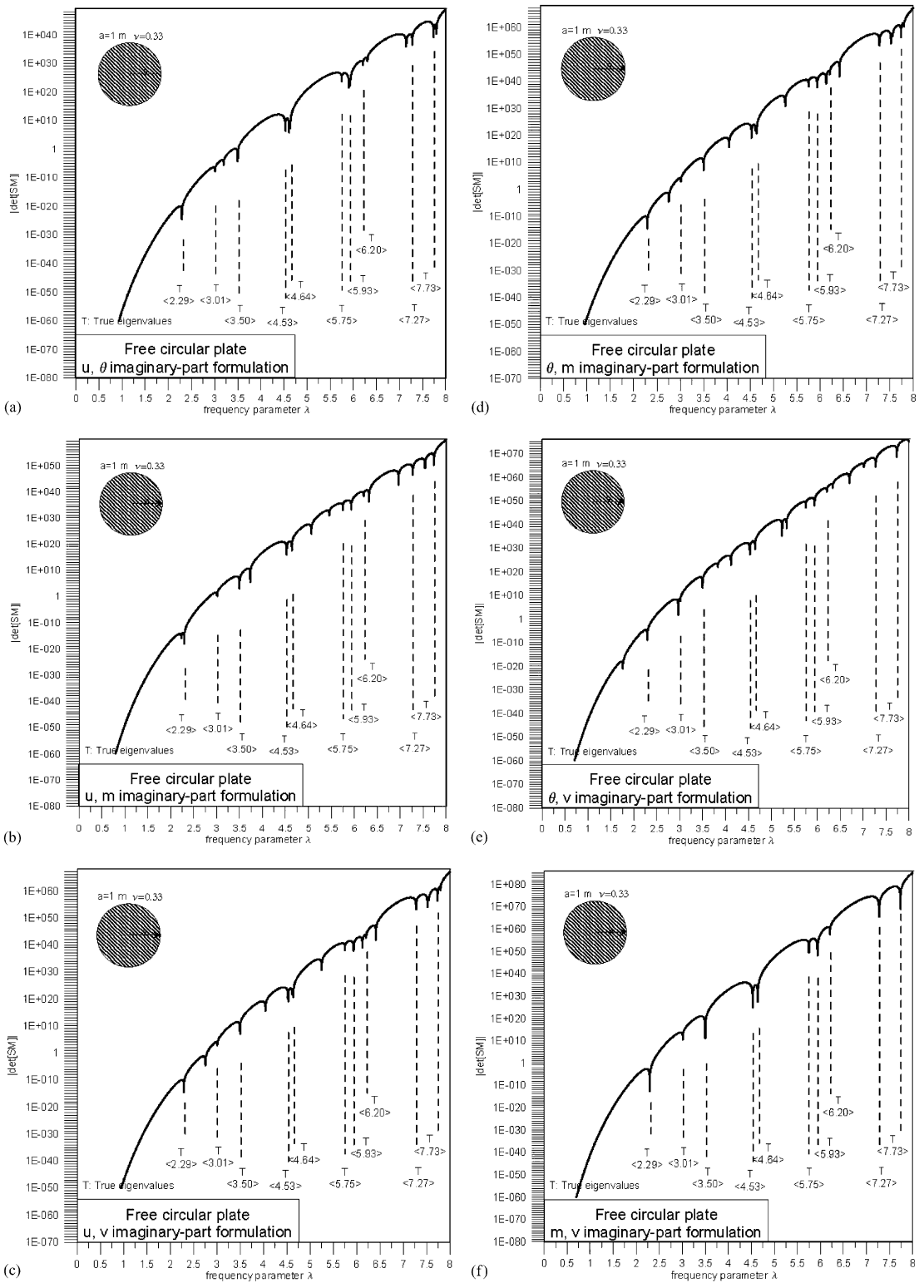

Fig. 4. The absolute value of determinant for $[SM^f]$ versus frequency parameter λ for the free circular plate using the six imaginary-part formulations.

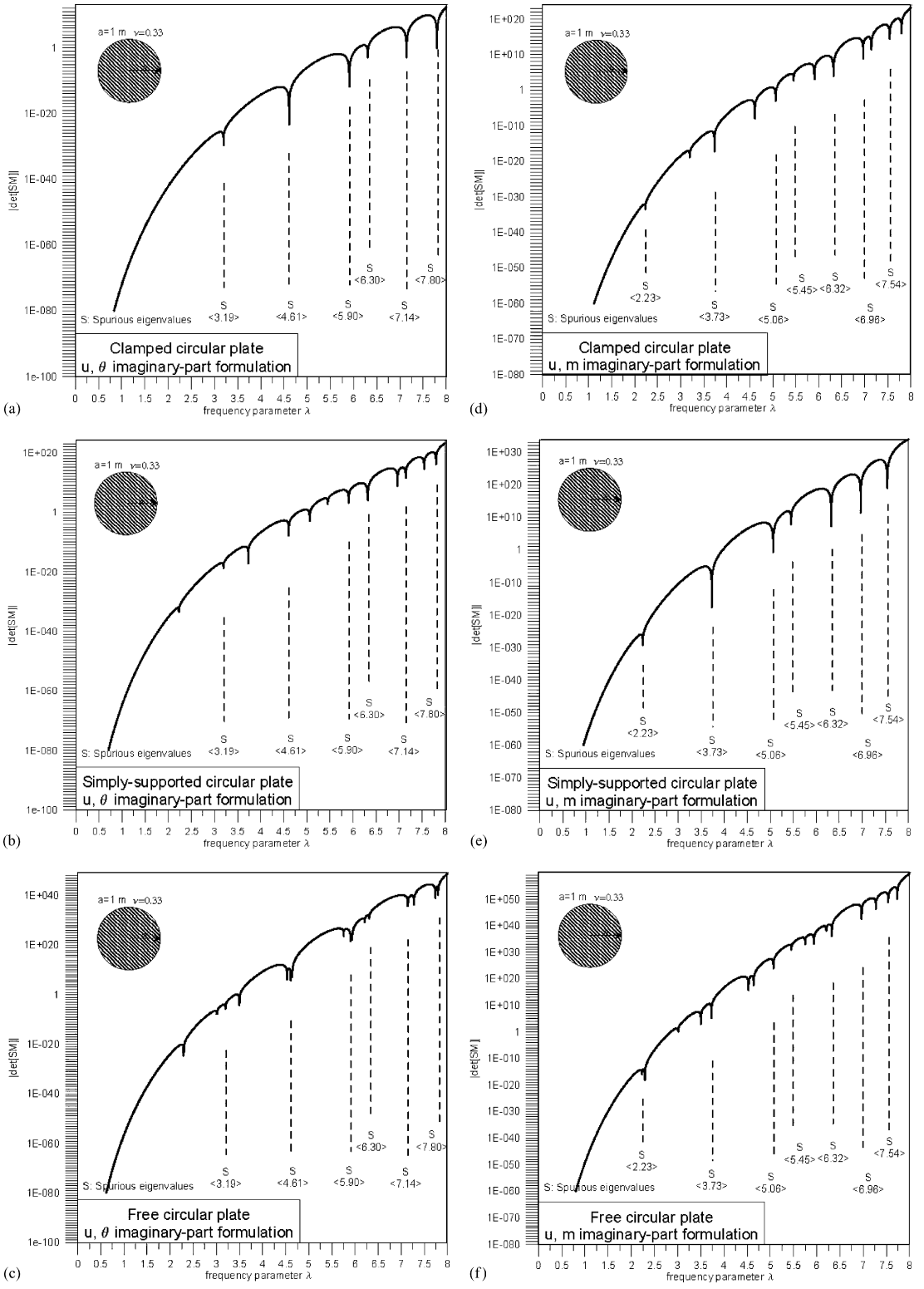

Fig. 5. The absolute value of determinant for [SM] versus frequency parameter λ using the imaginary-part formulation (u, θ or u, m formulation) to solve plates with different boundary conditions.

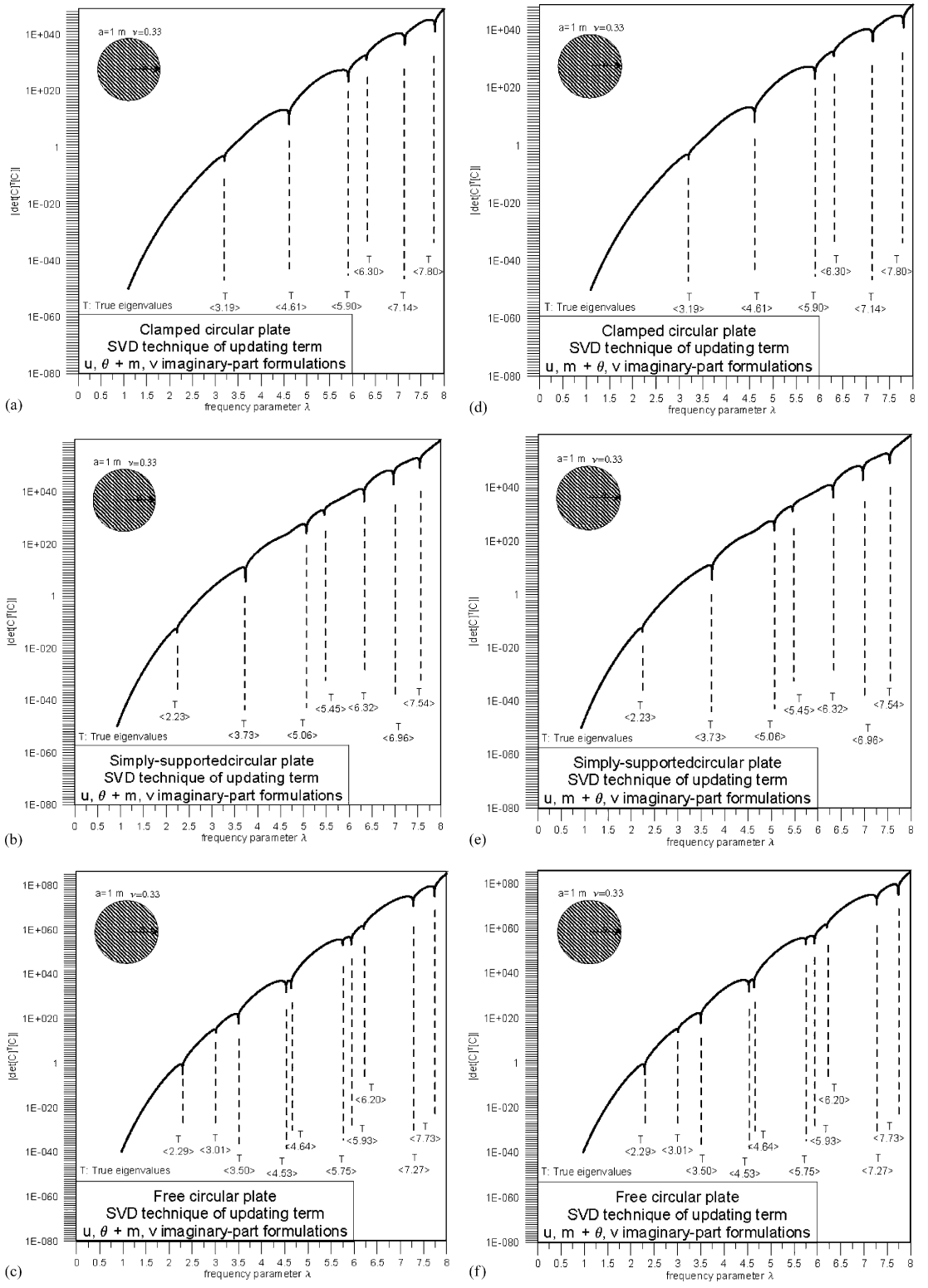

Fig. 6. The absolute value of determinant for the matrix $[C]^T[C]$ versus frequency parameter λ for the clamped, simply-supported and free circular plates by using the imaginary-part formulations with the SVD technique of updating term.

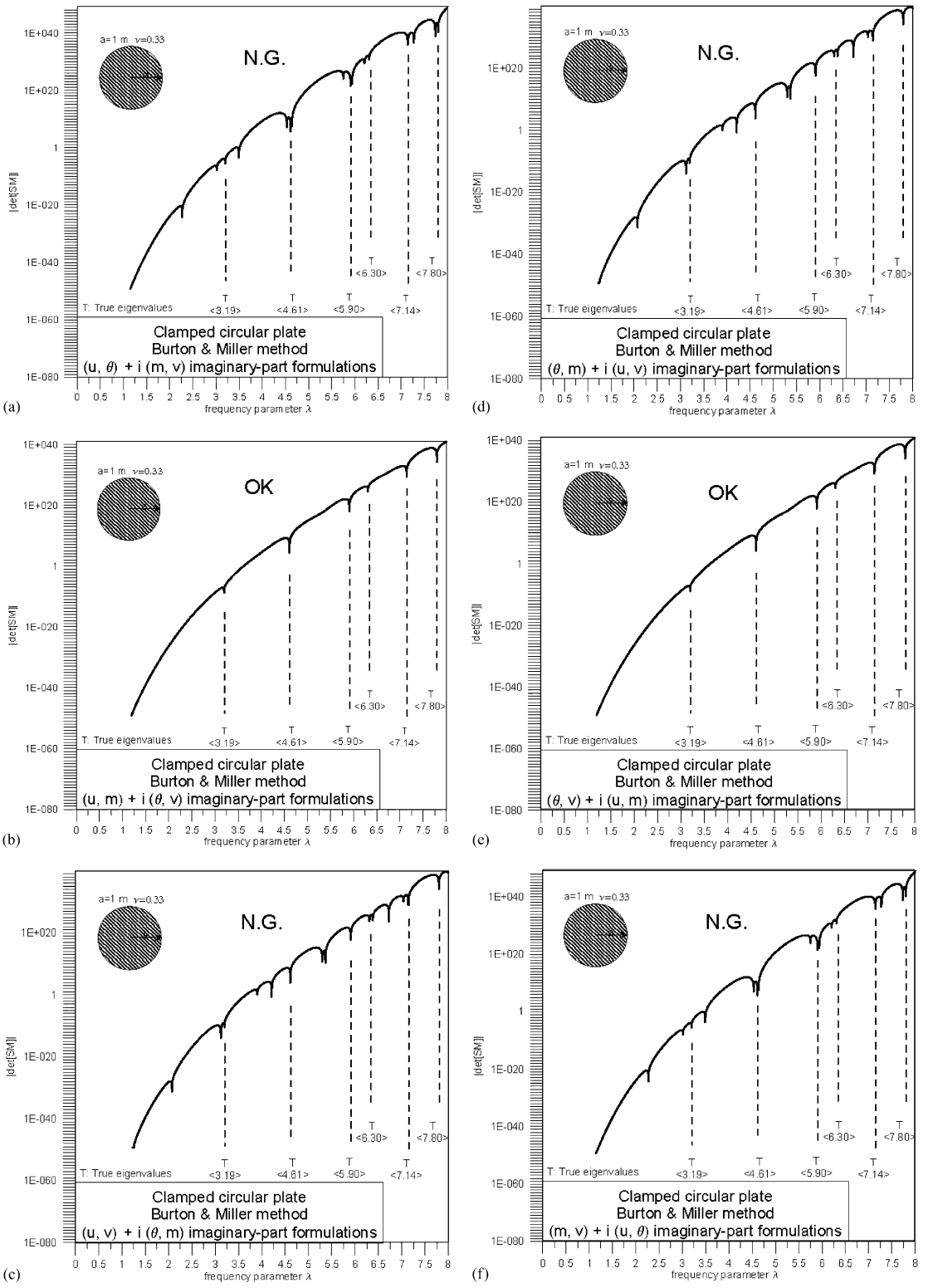

Fig. 7. The absolute value of determinant for the [SM^c] versus frequency parameter λ for the clamped circular plate using the six imaginary-part formulations in conjunction with the Burton and Miller concept.

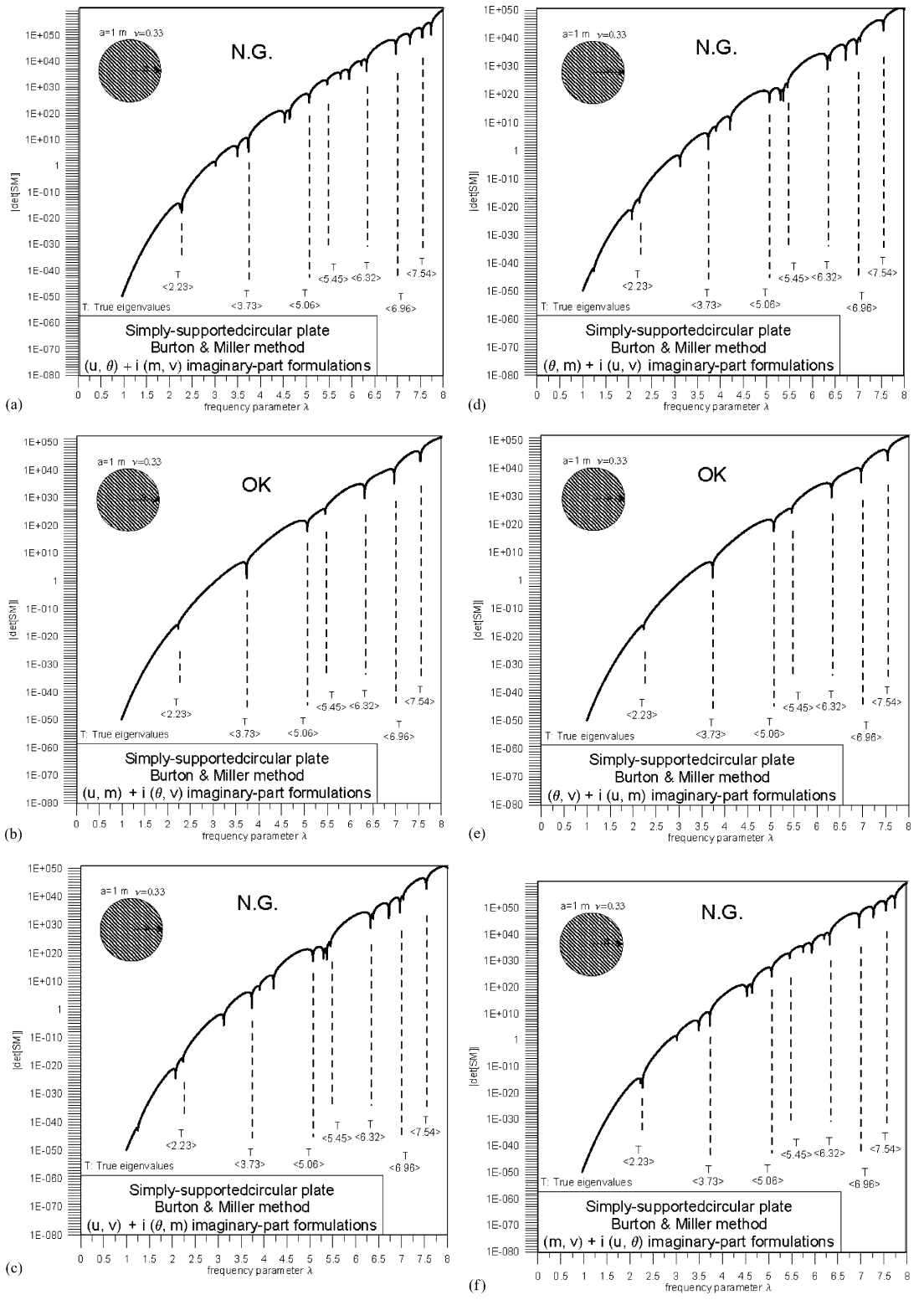

Fig. 8. The absolute value of determinant for the $[SM^s]$ versus frequency parameter λ for the simply-supported circular plate using the six imaginary-part formulations in conjunction with the Burton and Miller concept.

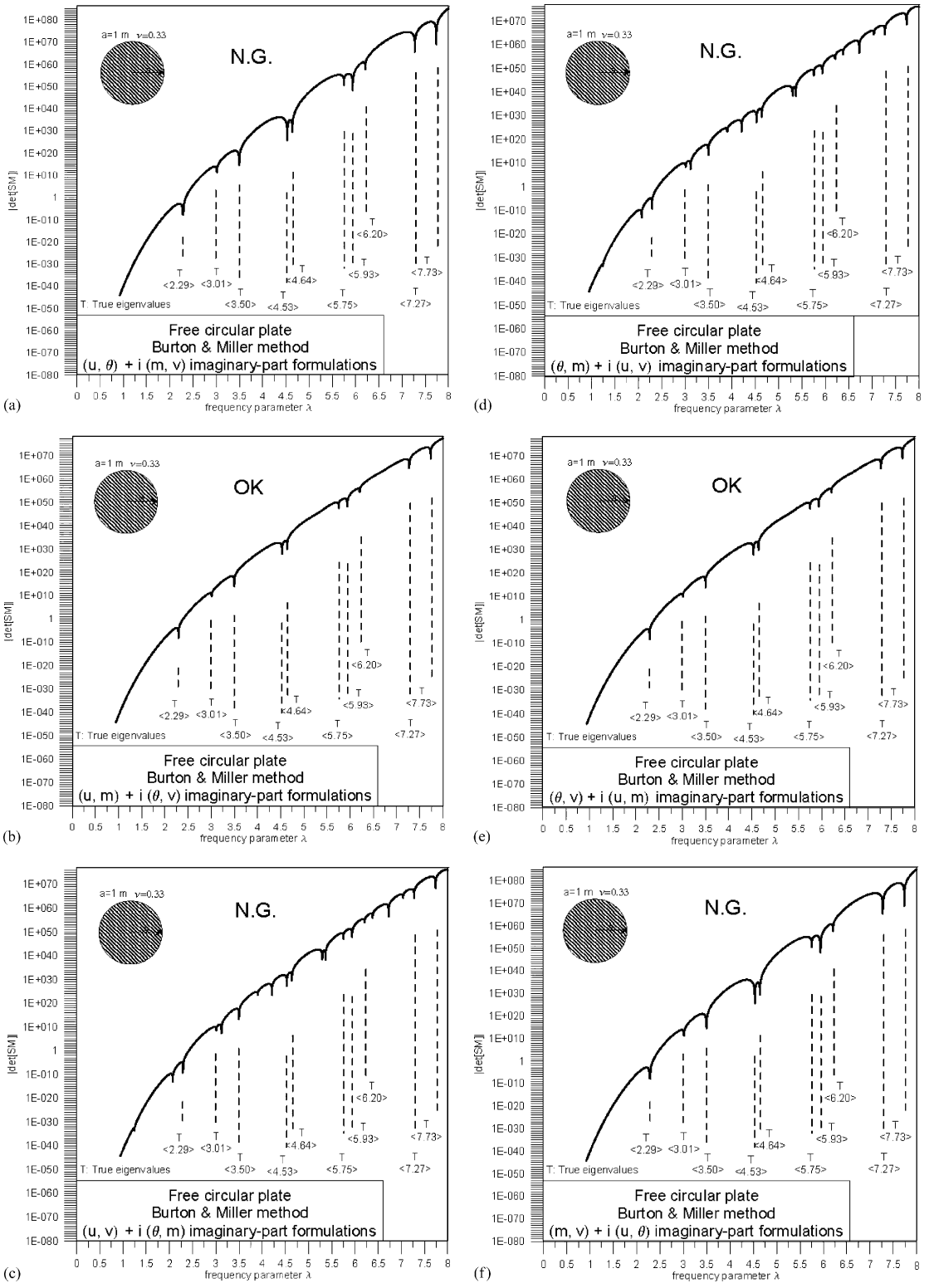

Fig. 9. The absolute value of determinant for the $[SM^f]$ versus frequency parameter λ for the free circular plate using the six imaginary-part formulations in conjunction with the Burton and Miller concept.

that the true eigenvalues depend on the specified boundary condition (C, S and F) instead of the six formulations (a, b, c, d, e and f). The spurious eigenvalues are embedded in each formulation as shown in Figs. 2–4, which satisfy the spurious characteristic equations in Table 2. In order to distinguish the spurious eigenvalues, Figs. 5(a)–(f) show the determinant of [SM] versus λ using the formulation (e.g., u, θ and u, m formulation) to solve the circular plates subject to different boundary conditions. It is found that any one of the clamped, simply-supported and free cases results in the same spurious eigenvalues, once we use the formulation (a, b and c—u, θ formulation; d, e and f—u, m formulation). The numerical results reconfirm that the occurrence of spurious eigenvalues only depends on the formulation instead of the specified boundary condition. All the spurious characteristic equations in the imaginary-part BEM are summarized in Table 2. The numerical results of the true eigenvalues agree well with the data in the Leissa book [20].

4.1.2. Treatment by using the SVD updating technique

Figs. 6(a)–(f) show the determinant of the $[C]^{\mathrm{T}}[C]$ versus λ for the clamped, simply-supported and free circular plates using the six imaginary-part formulations in conjunction with the SVD technique of updating term. Only the true eigenvalues are obtained without contamination of the spurious eigenvalues. Good agreement is made.

4.1.3. Treatment by using the Burton and Miller method and the complex-valued BEM

Figs. 7–9 show the determinant of the [SM] versus λ for the clamped, simply-supported and free circular plates using the six imaginary-part formulations in conjunction with the Burton and Miller concept. The failure cases are shown in the (a), (c), (d) and (f) cases as predicted in Table 3. The spurious characteristic equations of u, θ and m, v formulations are imbedded in the term $A(\lambda)$ by using the combination of u, θ and m, v formulation, and the spurious characteristic equation of m, v formulations is the same with the true characteristic equation of the free circular plate. The true and spurious eigenvalues are very close in the range $(0<\lambda<8)$ by using u, θ and m, v formulations in conjunction with the Burton and Miller concept. Only the combination of u, m and θ, v formulations can obtain the true eigenvalues in Figs. 7(b), 7(e), 8(b), 8(e), 9(b) and 9(e) as predicted in Table 3, since $A(\lambda)$ and $B(\lambda)$ cannot be zero at the same time. For the case by using the u, θ formulations in conjunction the m, v formulations after multiplying an imaginary number for solving the circular plates subject to different boundary conditions (Figs. 6(a), 7(a) and 8(a)), the spurious eigenvalues occur since $A(\lambda)$ may be zero for the spurious eigenvalues and $B(\lambda)$ is always zero in Table 3.

For the clamped, simply-supported and free circular cases, all the numerical results of the eigenvalues agree well with the data in Ref. [20] by using the SVD technique of updating term and the Burton and Miller method (u, m and θ, v formulations). All the true eigenvalues are shown in Tables 4–6 for clamped, simply-supported and free plates, respectively.

4.2. Rectangular plate subject to clamped boundary condition

A rectangular plate with length ($a = 1.2\,\mathrm{m}$) and width ($b = 0.9\,\mathrm{m}$) for the clamped boundary condition is considered. According to the imaginary-part BEM implementation, the boundary is discretized into 16

Table 4
True eigenvalues (λ) for the clamped circular plate ($a = 1$)

m	λ for values of n					
	0	1	2	3	4	5
0	3.19	4.61	5.90	7.14	8.34	9.52
1	6.30	7.80	9.19	10.53	11.83	13.10
2	9.44	10.95	12.40	13.79	15.15	16.47
3	12.57	14.10	15.58	17.00	18.39	19.75
4	15.71	17.25	18.74	20.19	21.60	22.99

Here n refers to the number of nodal diameters and m is the number of nodal circles, not including the boundary circle.

Table 5
True eigenvalues (λ) for the simply-supported circular plate ($a = 1$, $v = 0.33$)

m	λ for values of n					
	0	1	2	3	4	5
0	2.23	3.73	5.06	6.32	7.54	8.73
1	5.45	6.96	8.37	9.72	11.03	12.31
2	8.61	10.14	11.59	12.98	14.34	15.67
3	11.76	13.29	14.77	16.20	17.59	18.96
4	14.90	16.45	17.94	19.39	20.81	22.20

Here n refers to the number of nodal diameters and m is the number of nodal circles, not including the boundary circle.

Table 6
True eigenvalues (λ) for the free circular plate ($a = 1$, $v = 0.33$)

m	λ for values of n					
	0	1	2	3	4	5
0			2.29	3.50	4.64	5.75
1	3.012	4.53	5.93	7.27	8.56	9.82
2	6.20	7.73	9.18	10.57	11.93	13.25
3	9.37	10.91	12.38	13.80	15.19	16.55
4	12.52	14.06	15.55	17.00	18.42	19.81

Here n refers to the number of nodal diameters and m is the number of nodal circles, not including the boundary circle.

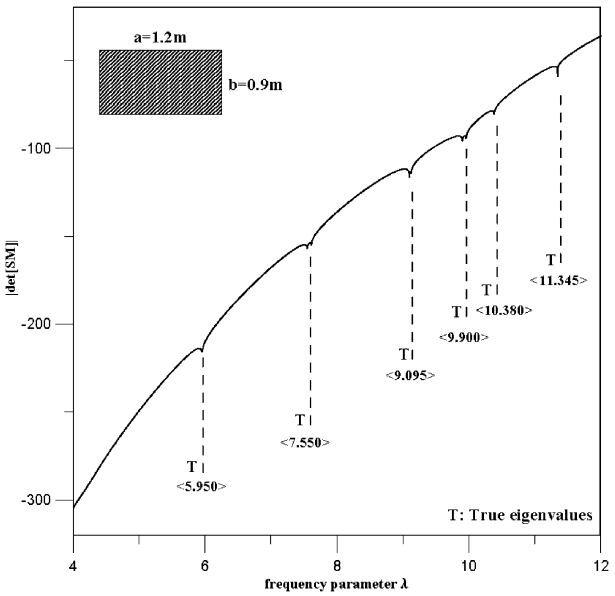

Fig. 10. The absolute value of determinant versus frequency parameter λ for the clamped rectangular plate using imaginary-part formulation.

constant elements. Although $6(C_2^4)$ options of the formulation can be considered, we used the $u-\theta$ formulation for illustration. Fig. 10 shows the true and spurious eigenvalues of the rectangular plate subject to the clamped boundary condition. After comparing with the results using different approaches [24,25], agreement is made as shown in Table 7. The conclusions are the same as the circular case that spurious

Table 7
The former six eigenvalues for the clamped rectangular plate using different approaches

	λ_1	λ_2	λ_3	λ_4	λ_5	λ_6
Dickinson [22]	5.964	7.730	9.151	9.975	10.30	11.99
ANSYS (441 nodes)	5.946	7.701	9.114	9.938	10.24	11.91
ANSYS (961 nodes)	5.950	7.706	9.123	9.948	10.26	11.94
Kang and Lee [23]	5.952	7.703	9.131	9.955	10.27	11.95
Present method (16 elements)	5.950	7.550	9.095	9.900	10.380	11.345

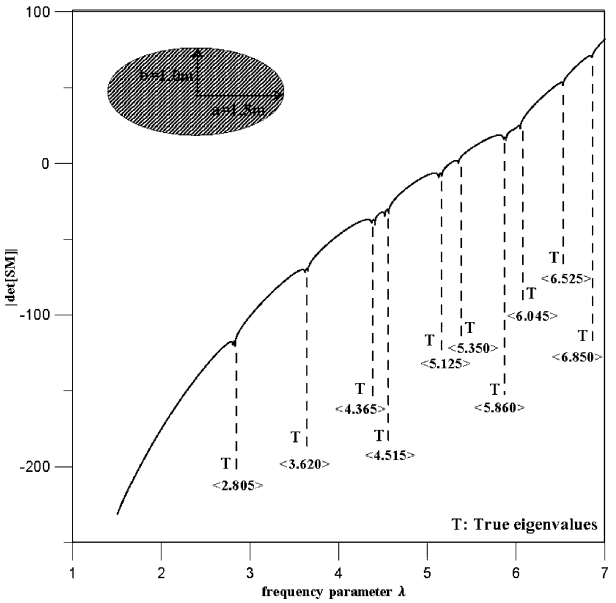

Fig. 11. The absolute value of determinant versus frequency parameter λ for the clamped elliptical plate using imaginary-part formulation.

Table 8
The former two eigenvalues for the clamped elliptical plate using different approaches

	λ_1	λ_2
Blevins [24]	2.751	3.706
Present method (14 elements)	2.805	3.620

eigenvalues happen to be the true eigenvalues for the clamped boundary condition if $u-\theta$ imaginary-part BEM is adopted.

4.3. Elliptical plate subject to clamped boundary condition

An elliptical plate with a semi-major axis ($a = 1.5$ m) and a semi-minor axis ($b = 1.0$ m) for the clamped boundary condition is considered. According to the imaginary-part BEM implementation, the boundary is discretized into 14 constant elements. Although $6(C_2^4)$ options of the formulation can be considered, we used the $u-\theta$ formulation. Fig. 11 shows the true and spurious eigenvalues of the elliptical plate subject to the clamped boundary condition. After comparing with the former two eigenvalues in Ref. [26], the results are acceptable as shown in Table 8.

5. Concluding remarks

The imaginary-part BEM formulations have been derived for the free vibration of plates. For a circular plate, the true and spurious solutions were analytically derived by using the degenerate kernel, Fourier series and circulants in the continuous and discrete systems. The eigenvalues were determined numerically for noncircular cases. Since any two equations in the plate formulation (four equations) can be chosen, C_2^4 (6) options were considered. The occurrence of spurious solution only depends on the formulation instead of the specified boundary condition, while the true solution is independent of the formulation and is relevant to the specified boundary condition. Three cases were demonstrated analytically and numerically to see the validity of the present method. Two alternatives (SVD updating technique and the Burton and Miller method) were adopted to suppress the occurrence of the spurious eigenvalues in the imaginary-part BEM. The SVD technique of updating term and the Burton and Miller method (u, m and θ, v formulations) can obtain the true eigenvalues and the results agree well with the Leissa's data [20]. Although the circular case lacks generality, it leads significant insight into the occurring mechanism of true and spurious characteristic equation. Here, the proof is only limited to the circular case, it is a great help to the researchers who may require analytical explanation to understand why the spurious characteristic equation occurs. The same algorithm in the discrete system can be applied to solve arbitrarily-shaped plate numerically without any difficulty. Nevertheless, mathematical derivation in the continuous and discrete systems cannot be done analytically. To demonstrate the validity of the present formulation for noncircular cases, rectangular and elliptical plates were verified by developing a general-purpose program.

References

[1] S.R. Kuo, J.T. Chen, C.X. Huang, Analytical study and numerical experiments for true and spurious eigensolutions of a circular cavity using the real-part dual BEM, *International Journal for Numerical Methods in Engineering* 48 (2000) 1404–1422.
[2] G. De Mey, Calculation of the Helmholtz equation by an integral equation, *International Journal for Numerical Methods in Engineering* 10 (1976) 59–66.
[3] G. De Mey, A simplified integral equation method for the calculation of the eigenvalues of Helmholtz equation, *International Journal for Numerical Methods in Engineering* 11 (1977) 1340–1342.
[4] M. Yas'ko, BEM with the real-valued fundamental solutions for the Helmholtz equation, *Proceedings of Seventh International Congress on Sound and Vibration*, Germany, 2000, pp. 2037–2044.
[5] J.R. Hutchinson, Determination of membrane vibrational characteristics by the boundary-integral equation method, in: C.A. Brebbia (Ed.), *Recent Advances in Boundary Element Methods*, Pentech Press, London, 1978, pp. 301–315.
[6] J.R. Hutchinson, G.K.K. Wong, The boundary element method for plate vibrations, *Proceedings of the ASCE Seventh Conference on Electronic Computation*, ASCE, St. Louis, Missouri, New York, 1979, pp. 297–311.
[7] J.R. Hutchinson, An alternative BEM formulation applied to membrane vibrations, in: C.A. Brebbia, G. Maier (Eds.), *Boundary Elements*, vol. VII, Springer, Berlin, 1985.
[8] J.R. Hutchinson, Analysis of plates and shells by boundary collocation, in: D.E. Beskos (Ed.), *Boundary Elements Analysis of Plates and Shells*, Springer, Berlin, 1991.
[9] R.P. Shaw, Boundary integral equation methods applied to wave problems, in: P.K. Banerjee, R.P. Shaw (Eds.), *Developments in Boundary Element Methods*—1, Applied Science Publishers, Barking, 1979.
[10] J.R. Hutchinson, Vibration of plates, in: C.A. Brebbia (Ed.), *Boundary Elements*, vol. X, Springer, Berlin, 1988.
[11] J.T. Chen, S.R. Kuo, Y.C. Cheng, On the true and spurious eigensolutions using circulants for real-part dual BEM, IUTAM/IACM/IABEM Symposium on Advanced Mathematical and Computational Mechanics Aspects of Boundary Element Method, Kluwer Press, Cracow, Poland, 2000.
[12] J.T. Chen, Recent development of dual BEM in acoustic problems, *Computer Methods in Applied Mechanics and Engineering* 188 (3–4) (2000) 833–845.
[13] J.R. Chang, W. Yeih, J.T. Chen, Determination of natural frequencies and natural modes using the dual BEM in conjunction with the domain partition technique, *Computational Mechanics* 24 (1) (1999) 29–40.
[14] J.T. Chen, C.X. Huang, K.H. Chen, Determination of spurious eigenvalues and multiplicities of true eigenvalues using the real-part dual BEM, *Computational Mechanics* 24 (1) (1999) 41–51.
[15] I.L. Chen, J.T. Chen, S.R. Kuo, M.T. Liang, A new method for true and spurious eigensolutions of arbitrary cavities using the CHEEF method, *Journal of Acoustical Society of America* 109 (2001) 982–999.
[16] Y. Niwa, S. Kobayash, M. Kitahara, Determination of eigenvalues by boundary element methods, in: P.K. Banerjee, R.P. Shaw (Eds.), *Developments in Boundary Element Method*—2, Applied Science Publishers, Barking, 1982.
[17] J.T. Chen, J.H. Lin, S.R. Kuo, S.W. Chyuan, Boundary element analysis for the Helmholtz eigenvalue problems with a multiply connected domain, *Proceedings of the Royal Society Series A* 457 (2001) 2521–2546.

[18] J.T. Chen, L.W. Liu, H.-K. Hong, Spurious and true eigensolutions of Helmholtz BIEs and BEMs for a multiply-connected problem, *Proceedings of the Royal Society Series A* 459 (2003) 1891–1924.
[19] M. Kitahara, *Boundary Integral Equation Methods in Eigenvalue Problems of Elastodynamics and Thin Plates*, Elsevier, Amsterdam, 1985.
[20] A.W. Leissa, *Vibration of Plates*, American Institute of Physics, 1993.
[21] J.T. Chen, C.S. Wu, K.H. Chen, Y.T. Lee, Degenerate scale for the analysis of circular thin plate using the boundary integral equation method and boundary element method, *Computational Mechanics* (2005), in press.
[22] J.T. Chen, M.H. Chang, K.H. Chen, S.R. Lin, The boundary collocation method with meshless concept for acoustic eigenanalysis of two-dimensional cavities using radial basis function, *Journal of Sound and Vibration* 257 (4) (2002) 667–711.
[23] A.J. Burton, G.F. Miller, The application of integral equation methods to numerical solution of some exterior boundary value problems, *Proceedings of The Royal Society Series A* 323 (1971) 201–210.
[24] S.M. Dickinson, The buckling and frequency of flexural vibration of rectangular, isotropic and orthotropic plates using Rayleigh's method, *Journal of Sound and Vibration* 61 (1978) 1–8.
[25] S.W. Kang, J.M. Lee, Free vibration analysis of arbitrary shaped plates with clamped edges using wave-type functions, *Journal of Sound and Vibration* 242 (1) (2001) 9–26.
[26] R.D. Blevins, *Formulas for Natural Frequency and Mode Shape*, Robert E. Krieger, Malabar, FL, 1984.